7 Magnetic confinement fusion: stellarator

[H. Wobig, F. Wagner]

7.1 Introduction

The stellarator is one of the earliest confinement concepts in fusion research. Since its proposal by L. Spitzer [58Spi] this line has experienced many changes and modifications, and a large variety of experiments has explored the plasma behavior using various heating methods. The main argument in favor of stellarators is their potential as a steady-state fusion reactor, an argument which is gaining more and more weight in current fusion reactor studies.

The stellarator system offers a distinct alternative to the mainline approaches to magnetic fusion power and has several potentially major advantages which are summarized in Table 7.1. The steady-state magnetic fields simplify superconducting magnet design, remove the need for pulsed superconducting coils, and eliminate energy storage required to drive pulsed coils. Plasma confinement during start-up is aided by the presence of magnetic surfaces at all times during this phase. Steady-state plasma operation at ignition is a clear potential advantage of the stellarator concept. Such operation would simplify blanket design, since fatigue problems would be eliminated. Steady-state operation, however, implies a need to refuel the plasma continually. Also, impurity control and ash removal are needed for steady-state burn, and several options exist to achieve both requirements. The stellarator configuration naturally possesses a magnetic limiter and a helical divertor, which can be used to advantage for impurity control. In modern advanced stellarators the same goal can be achieved by the island divertor.

Table 7.1. Main features of a stellarator reactor.

Steady-state magnetic fields.
Steady-state plasma operation at ignition or high Q.
No energy storage and low re-circulating power requirements.
Moderate plasma aspect ratio (8…12) which can improve access.
Start-up on existing magnetic surfaces with confinement at all times
No significant positioning or field shaping coils.
No major disruptions that could lead to an energy dump on the first wall.
Several potential methods for impurity control and ash removal.
No net toroidal current in the plasma required.

A stellarator can have a relatively high aspect ratio and does not require expensive complicating auxiliary magnets (e.g. Ohmic heating, field shaping, and position control coils). Its coil configuration permits access to the device from all sides and facilitates a modular approach to blanket and shield design. Since stellarators and torsatrons can operate free of net toroidal current and do not exhibit major plasma disruptions, the major concern of an excessive energy dump on the first wall can be eliminated for the reactor.

In order to make an effective reactor, it is necessary that the plasma achieve certain basic conditions, as reflected by the parameters $n\tau$, T_e, T_i and β. These conditions are in turn governed by the magnetic parameters chosen for the reactor, as reflected by the rotational transform, shear, well depth, aspect ratio and harmonic content of the surfaces. In turn, these magnetic parameters are affected by the choice of the magnetic coil configuration used. The coupling between plasma performance, magnetic topology and magnet design is particularly intimate and flexible for the stellarator configuration, leading to a wide range of potential reactor options.

The question of operational mode for any magnetically confined fusion reactor is centered around the following issues: pulsed versus steady-state plasma; driven high-Q versus ignited operation; refueling mechanism; impurity-control scheme; and plasma start-up and rundown procedure. The uniqueness of the stellarator in this respect rests with the generation of the full magnetic field topology solely by external currents.

7.2 Survey of stellarator reactor studies

Early stellarator reactor designs [54Spi, 58Spi, 61Mil, 69Gib, 70Col, 71Gib, 78Miy] concluded that the coupled problems of high coil cost and low system power density (i.e. low beta) were particularly severe for the classical stellarator. The more recent torsatron [71Gou, 79Pol] and modular-coil configurations [72Wob, 81Mil], however, show strong promise in alleviating the coil problem per se. For these reasons, the overall coil performance represents a major element in the more recent reactor survey and systems analyses [72Wob].

The first stellarator reactor, the Princeton Model-D design [58Spi], represents one of the most comprehensive extrapolations of a confinement concept to the reactor stage. Experimental and theoretical work during the 1950s, however, established that several of the physics and technology assumptions upon which the Model-D design was based were untenable (e.g., average beta of 0.75, "figure-8" topology and copper coils) [58Spi, 62Mil]. The Model-D design, however, set a precedent for stellarator-like reactors that was prominent until the publication of the T-1 torsatron design [71Gou]: the tendency for stellarators to produce large amounts of thermal power (i.e. > 5 GW). Attempts to impose equilibrium and stability limits on beta led to reactor survey calculations at Culham [78Miy, 69Gib]. The assumed scaling of beta with plasma aspect ratio (equilibrium limit) in toroidal geometry, when coupled with the conservative transport scaling assumed, resulted in systems with high peak magnetic field strengths in the inboard region of the coils. Three additional stellarator reactor designs, given in [71Gou, 79Pol, 72Wob], invoke the torsatron coil configuration. The Heliotron C design [74Iiy] is based upon a large beta value, which in a system of large major radius also leads to large power output. This situation exists for the Kharkhov design point [76Geo].

The MIT T-1 torsatron design [71Gou] reflects an attempt to reduce the total (thermal) power output to < 4 GW under the assumption of conservative beta limits. The assumed Alcator (empirical) transport scaling allows moderate on-axis field strength, and the large aspect ratio reduces the corresponding peak field on the inboard region of the coil. Because of the monolithic helical coils required for this $l = 3$ torsatron reactor, modularity could be achieved only by proposing demountable superconducting breaks within the coil structure and modules that weigh of the order of 1000 t.

The UWTOR-M reactor [82Bad], designed at the University of Wisconsin, is one of the first devices utilizing the concept of modular coils. The magnetic field is generated by 18 modular coils, no further coils for plasma control are needed. The natural stellarator divertor is used for impurity control in conjunction with high performance divertor targets. The idea is to collect the power on rotating target plates of cylindrical shape and to recover the energy at high temperature thus improving the power balance of the reactor. The thermal output of the reactor is rather large (5500 MW), which results from the choice of a 6-field-period configuration with aspect ratio 14 and the necessity to make the device large enough to accommodate a breeding blanket and a shield. These requirements unavoidably lead to a large plasma volume. The modular stellarator reactor (MSR) developed at the Los Alamos Laboratories is a classical $l = 2$, $m = 6$ configuration generated by 24 modular coils. The thermal output is of the order of 4000 MW. The main aspect of the MSR study is to elucidate the impact of the reactor point design on the engineering features of the modular coils.

The study on the modular stellarator ASRA6C (see Fig. 7.1) was carried through in 1987 as a joint effort of IPP Garching, FZK Karlsruhe and the University of Wisconsin [87Boe1]. The basis of this study was the magnetic field configuration of Wendelstein 7-AS and the aim was directed towards the clarification of critical issues of an advanced modular stellarator reactor and was not meant as a point design. Neglecting physics issues as critical β-limits, neoclassical transport, bootstrap currents etc., main emphasis was concentrated on technical issues, mainly superconducting coils, blanket, shield and maintenance.

A scoping study considered reactors of various dimensions with a major radius ranging from 15 m to 25 m. The parameters of the reference case are listed in Table 7.3.

A characteristic feature of the ASRA6C coil system is the elliptic bore of the coils which is the same in all coils leading to the same elliptical shape of blanket and shield elements. This principle has already been applied to the Wendelstein 7-AS device where the cross section of the vacuum tube is elliptic. In the reactor the consequence of this geometry is that removable blanket elements can easily be replaced. The concept of maintenance is based on demountable joints between coils and the radial displacement of one sector of the coil system. Blanket, first wall and divertor units are then replaced from both sides of the modules. The critical issue of this procedure is the demounting of the inter-coil support elements, which are at cold temperature. Engineering studies in FZK proposed a solution of this problem.

The MHH is a 4-period modular stellarator reactor, which has been designed in a joint effort by a group of fusion laboratories in the USA [97UCS]. The approach is similar to that used in the ARIES-tokamak reactor studies: an integrated physics, engineering, reactor component and cost optimization. The same assumptions and algorithms are used to compare stellarator reactors with tokamak reactors. As in all stellarator reactors, a critical design constraint is to minimize the distance between plasma edge and coil inboard side consistent with adequate tritium breeding and sufficient shielding of the superconducting coils. Dimensions of the breeding blanket must be minimized, which results in a blanket concept with liquid lithium as breeder and coolant. To reduce MHD-losses of the liquid flowing across the magnetic field the cooling channels are coated with CaO. Low-activation vanadium alloys are envisaged as structural material. Although the thermal fusion power is only 2200 MW, high temperature in the cooling channels (610 °C) allows one to use a thermal cycle with high efficiency (46 %). A major aim of the power plant study was to make a cost comparison with the ARIES tokamak reactor. Based on the same assumptions and computational methods the study comes to the conclusion that a stellarator reactor with the size of MHH is cost-competitive with a tokamak reactor.

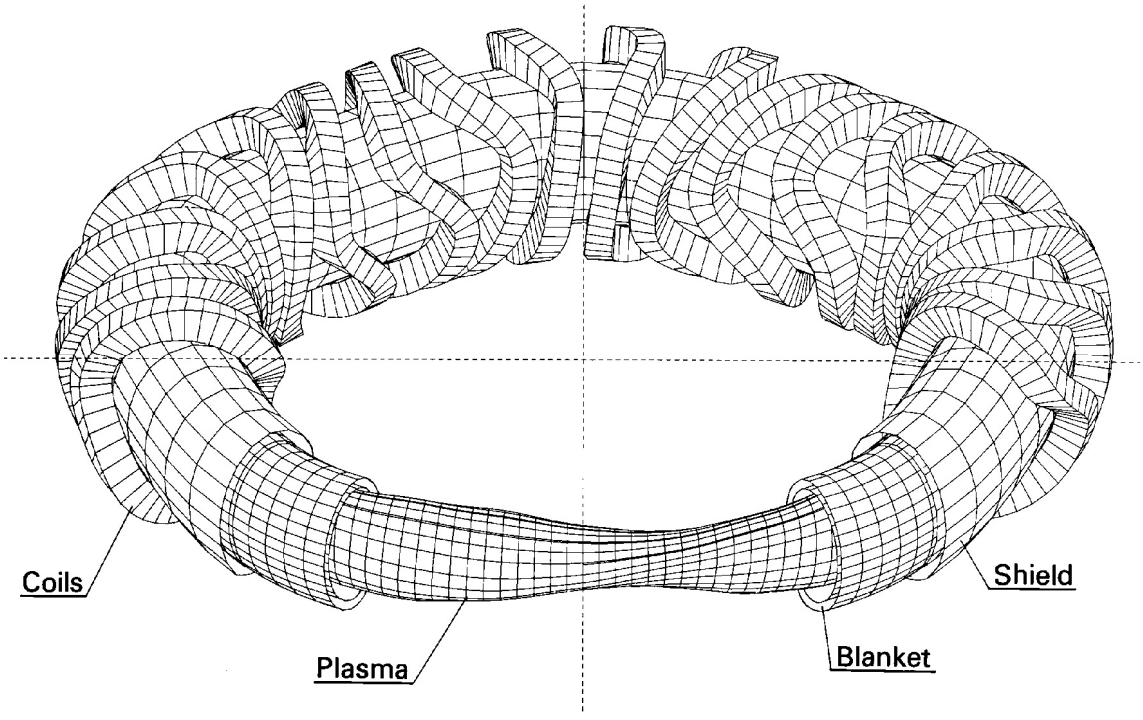

Fig. 7.1. ASRA6C. Schematic view of plasma, blanket, shield and coils.

Table 7.2. Main parameters of modular stellarator reactors.

		UWTOR-M	MSR
Major radius	[m]	24.1	20.2
Coil radius	[m]	4.77	4.58
Average plasma radius	[m]		1.84
Multi-polarity *l*		3	2
Field periods *m*		6	6
Number of coils		18	24
Coil current	[MA]	35	26.9
Field on axis	[T]	5.5	6.4
Maximum field on conductor	[T]	9.5	13
Magnetic energy	[GJ]	190	200
Average beta	[%]	5	4
Thermal output	[MW]	5500	4000

Table 7.3. Parameters of stellarator reactors.

		ASRA6C	MHH
Major radius	[m]	20	14
Average radius of coils	[m]	4.57	4
Coil current	[MA]	18	13.8
Number of modular coils		30	32
Average plasma radius	[m]	1.6	1.63
Number of field periods		5	4
Field on axis	[T]	5.3	5
Maximum field on coils	[T]	10.4	14.5
Magnetic energy	[GJ]	117	80
Average beta	[%]	5	5
Thermal output	[MW]	4000	2290

The Helias (Helical Advanced Stellarator) reactor is an upgraded version of the Wendelstein 7-X device taking into account the design criteria of a power reactor. The magnetic field of this device is a 5-period configuration with some optimized properties, which will be described in Sect. 7.3. These include reduced Pfirsch-Schlüter currents and the subsequent reduction of the Shafranov shift. The dimensions of a Helias reactor are determined by the following requirements:

– The magnetic configuration is similar to the configuration of Wendelstein 7-X.
– There must be sufficient space for blanket and shield.
– The magnetic field is small enough to allow for NbTi superconducting coils.
– Plasma confinement must be sufficiently good to provide ignition.
– Thermal fusion power should be about 3000 MW.

These requirements have led to the parameters of the Helias reactor [98Bei1] listed in Table 7.4. The coil system of a modular Helias reactor is displayed in Fig. 7.2.

Technical studies have been focused on the optimization of the coil system with respect to magnetic field distribution, forces and stresses using the ANSYS code. In a first survey several blanket concepts, developed for the DEMO tokamak, have been adapted to the Helias geometry. The minimum distance between first wall and coils is 1.3 m, which is sufficient to accomodate all blanket concepts which have been developed for tokamak reactors. A water-cooled LiPb-blanket is favored in comparison with ce-

ramic breeders, since safety properties and maintenance procedure seem to be more favorable within this concept. A self-cooled LiPb-blanket with He-cooling is an alternative, however, this concept requires the reduction of eddy currents and MHD losses by coating of the cooling tubes with insulators or by insulating inserts. Maintenance and replacement of blanket segments through portholes is consistent with the geometric constraints imposed by the coils and the inter-coil support system.

A characteristic feature of the modular Helias reactor is the large area of the first wall of the order of 2600 m^2. A neutron power of 2400 MW will yield an averaged neutron power density of less than 1 MW/m^2 and a peaking factor of 1.6. This feature provides an increase of the lifetime of first wall and blanket, however, a larger blanket has to be replaced than in a compact device.

Helical reactor design studies are based on the LHD concept, which has been developed at the National Institute of Fusion Studies (NIFS) in Toki, Japan. The LHD experiment is a torsatron with $l = 2$ helical windings and 10 field periods [90Iiy] and the advantage of the LHD concept is the natural divertor with two X-points, which helically encircles the plasma. Apart from this helical structure it has many features in common with the tokamak divertor. Two versions of the LHD-type reactor exist: the Force-Free Helical Reactor (FFHR [98Sag]) and the Modular Helical Reactor (MHR). The main feature of the FFHR is the arrangement of the helical windings in such a way that the forces on the helical windings are minimized. This requirement leads to an $l = 3$ system with 18 field periods. The minimum distance between plasma and helical coils, which is needed to accommodate a breeding blanket or at least a shielding blanket, is the most important design parameter determining the dimension of the reactor. For this reason the major radius of FFHR1 is 2 m. FFHR2 ($R = 10$ m, $l = 2$, $m = 10$) is a more compact version of the reactor and may be considered as an upgrade version of the LHD experiment (Table 7.5).

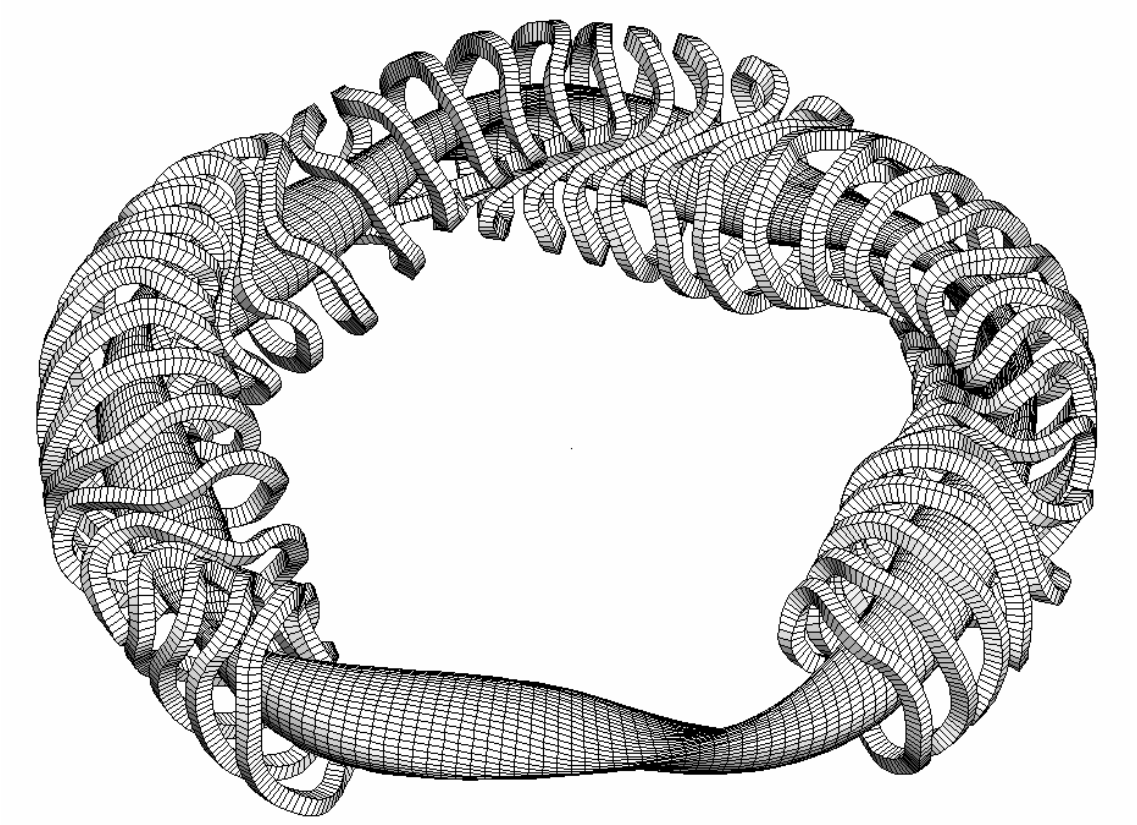

Fig. 7.2. Coil system and outer magnetic surface of a modular Helias reactor.

In FFHR design, molten salt FLIBE ($LiF\text{-}BeF_2$) has been selected as a self-cooling tritium breeder. There are safety aspects which favor this choice: low tritium solubility, low chemical reactivity with water and air, low pressure operation and low electric resistance. The space available for a blanket is rather narrow, not more than 1 m radial distance is left for blanket and shield, therefore shielding of the superconducting coils against neutron radiation is a critical issue. Large gaps between helical windings are an advantage of the torsatron systems; access to the blanket is easy and removal and replacement of blanket elements in the reactor should not be an issue.

Table 7.4. Main parameters of an advanced stellarator reactor of the Helias type.

Major radius	22.00 m
Minor radius	1.800 m
Average radius of coils	5.46 m
Number of coils	50
Coil current	10.8 MA
Plasma volume	1407 m^3
Iota(a)	1.000
Magnetic field on axis	5 T
Maximum field on coils	10.50 T
Stored magnetic energy	100 GJ
Beta(0)	15.67 %
Average beta	4.241 %
Fusion power	3000 MW

Table 7.5. Main parameters of Helical Reactors in comparison with the LHD experiment.

		LHD	FFHR1	FFHR2
Major radius	[m]	3.9	20	10
Plasma radius	[m]	0.65	2	1.2
Magnetic field	[T]	4	12	10
Average beta	[%]	5	0.7	1.8
Density $n(0)$	[m^{-3}]	1×10^{20}	2×10^{20}	2.8×10^{20}
Temperature $T(0)$	[keV]	10	22	27
Fusion power	[MW]		3000	1000
Polarity l		2	3	
Field periods		10	18	10
Stored magnetic energy	[GJ]	1.64	1290	147

7.3 Coil configurations

The most expensive component of the reactor core is the superconducting coil system. To confine plasma in a closed system with a toroidal field, it is necessary to provide a twist, or rotational transform, of the magnetic field lines. By suitable adjustment of the twist, nested closed toroidal magnetic surfaces can be obtained. This is accomplished in tokamaks by passing a toroidal current in the plasma to create a poloidal field. A stellarator can be defined as a device where this rotational transform is provided solely by coils outside the plasma so that steady-state operation can be achieved. Various coil systems to achieve this goal have been proposed in the past, a short survey will be given in he following.

The original stellarator-concept used the torsion associated with a non-planar magnetic axis, such as in a figure-eight shape, to provide this transform. It can be seen quite easily by following a magnetic field line around such a system that it returns at a rotated position on the same magnetic surface. The need for shear to stabilize MHD interchange instabilities led to the classical stellarator concept [58Joh], where the magnetic axis can be planar; the poloidal field is provided by a set of $2l$ toroidally continuous helical windings with current flowing in opposite directions in adjacent windings, and the toroidal field is obtained from currents in planar poloidal coils. The torsatron [70Gou] is a straightforward extension of this classical stellarator where the current goes in the same direction in the helical coils and provides both the poloidal and toroidal fields. The idea of deforming the poloidal coils either into an elliptic shape with a planar cross section [66Pop] or by warping so that they provide both components of the field has also evolved. All of these techniques for obtaining stellarator configurations with useful magnetic surfaces have considerable flexibility and many variations.

Classical stellarator coils suffered from two problems: the large, inwardly directed force acting on one set of the helical coils, and the interlinked geometry of the toroidal field coils and the helical windings. Both problems are alleviated in torsatrons where the access can also be improved. The forces on modular coils, both those associated with figure-eight geometries and with twisted coils, are not directed inwards towards the plasma. Thus a reasonable support structure, located outside and on the sides of the coils, is all that is required. The support structure required for steady-state operation of torsatrons, or of modular stellarators, is straightforward. The forces in these devices can be made comparable to or less than in a tokamak. Because of the larger aspect ratio envisioned in stellarators, the fields at the coils as well as the forces on them are reduced significantly.

7.3.1 Continuous coil stellarators

In continuous coil stellarators, the helical magnetic field necessary for closed magnetic surfaces is generated by windings which are themselves helical, linking the plasma in both toroidal and poloidal directions. The advantage of continuous helical windings lies in the fact that the strength of the helical component of the magnetic field is proportional to the largest helical component of the generating current. Continuous windings are separable into two categories, depending upon whether the helical windings are also used to generate a net toroidal magnetic field.

In the "classical" stellarator configuration, $2l$ windings ($l = 1, 2, 3, \ldots$) carrying currents in alternate directions are used to produce a stellarator field with l-fold poloidal symmetry without a net toroidal field. Therefore additional toroidal field coils are required. Figure 7.3 shows a schematic of an $l = 2$ stellarator. In all classical stellarators built thus far, the toroidal field coils are located outside of the helical windings, but this is not necessary in principle. Examples of existing classical stellarators are Wendelsein 7-A, CLEO, L-2, JIPP T-2, and many others. One of the advantages of the stellarator configuration is the flexibility associated with the possibility to vary the helical and toroidal field components independently. This feature allows a wide range of configurations in a single experimental device, and has made possible studies of the transition from tokamak-like configurations (rotational transform produced entirely or almost entirely by toroidal plasma currents) to pure stellarator configurations (with no net toroidal plasma current).

A particular disadvantage of the classical stellarator configuration arises from the interaction between the toroidal field coils and the helical windings. If the helices are imbedded in a large toroidal magnetic field, large radial forces appear, which alternate in direction from one helix to the next. Thus, for large devices with significant confining fields, the problem of supporting the helices becomes very serious, as relatively little space is available for structure. For one set of the helical windings the support structure must be placed under the coil, between it and the plasma. For a stellarator reactor this would make an economic design difficult. Since the field falls rapidly with decreasing radius, the coils must be near the plasma and this loss of space is indeed severe. Since the helical windings and the toroidal field coils are interlinked the disassembly and maintenance would be difficult.

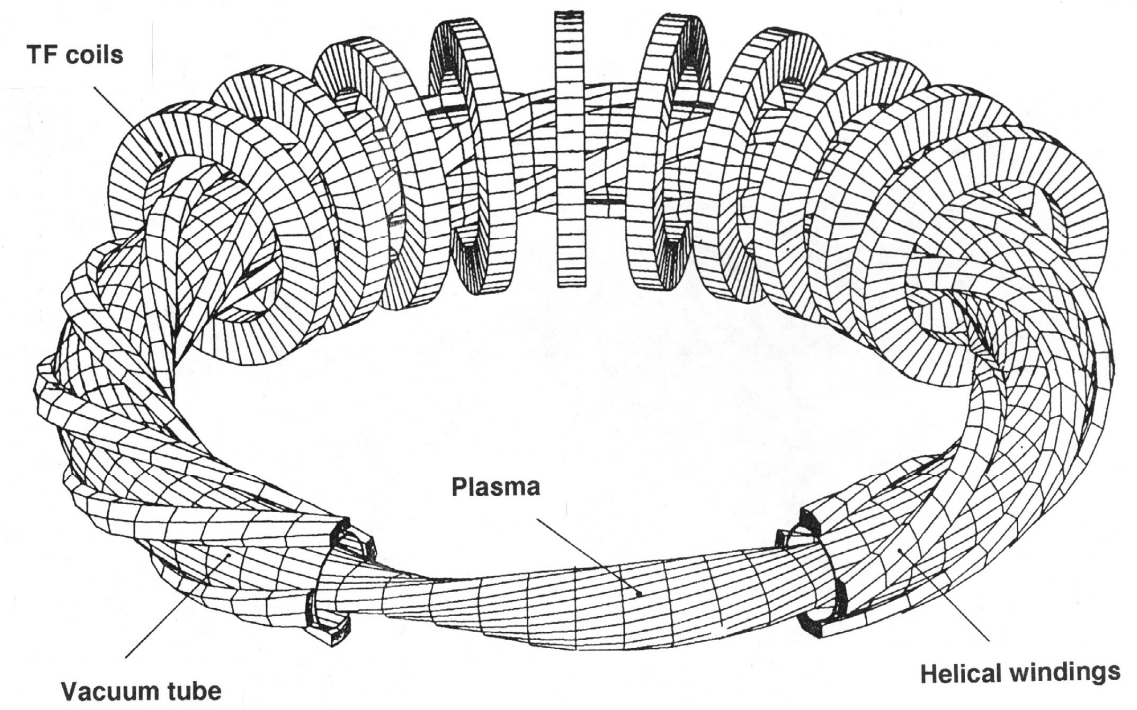

Fig. 7.3. Classical $l = 2$ stellarator Wendelstein 7-A. The current in adjacent helical windings flows in opposite direction. Below the helical windings: section of the vacuum tube.

7.3.2 Torsatron configurations

Some of these difficulties of the classical stellarator are alleviated in the torsatron configuration (see Fig. 7.4). Here, a field with l-fold poloidal symmetry is generated by l helical windings, all carrying current in the same direction. The torsatron thus generates both toroidal and poloidal field components, and, in principle, no other coils are needed. Furthermore, the complication with two sets of interwoven windings is eliminated. Problems associated with disassembly and maintenance still exist due to the toroidal continuity of the helical coils but are less severe. Since in torsatrons one set of l windings is used (rather than the $2l$ windings of a stellarator) the access can be improved.

The torsatron coils usually generate an average vertical field, which opens the vacuum flux surfaces. Thus, unless a specific winding law is selected (the "ultimate" torsatron law), an additional compensating vertical field coil set is needed. Furthermore, the basic torsatron configuration lacks experimental flexibility (i.e., variation of rotational transform, well depth, etc.), because of the use of a single set of windings. This flexibility can be restored with the use of an additional small vertical field, an additional small toroidal field or by allowing variation in the helical harmonic content.

Among the advantages of the torsatron configuration is the possibility of significant reduction of the forces on the helical windings. The forces tend to be directed radially outward, so that the support structure is no longer a severe problem. Indeed, it is possible to transfer the average outward forces onto external Helmholtz coils far from the plasma. For a torsatron with a certain winding law of the helical coils the radial force averaged over a field period may even be reduced to zero. For this case large forces appear on the compensation coils, but these can be located where there is adequate space for support structure.

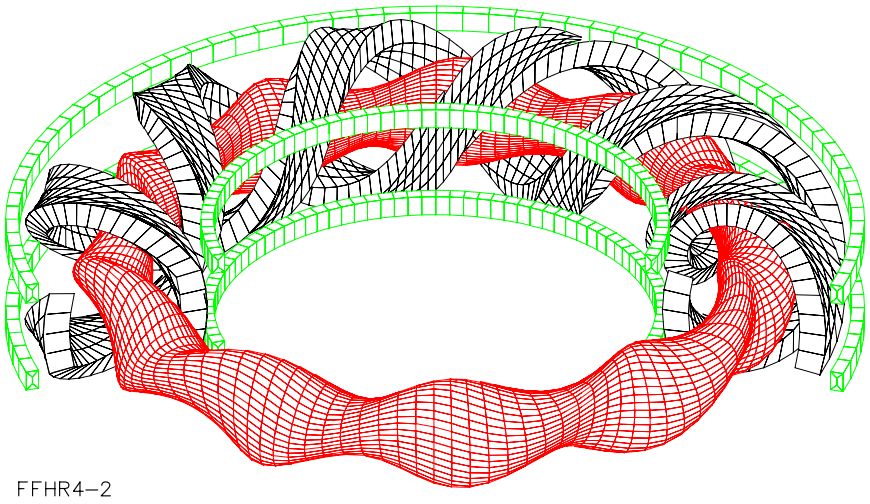

Fig. 7.4. Torsatron with unidirectional helical windings and circular return currents.

7.3.3 The Heliac concept

As in the figure-8 system the Heliac concept utilizes circular coils and shapes the plasma according to the requirements of equilibrium and stability; in particular, a magnetic well is realized , which did not exist in the original figure-8 configuration. This idea has lead to a configuration where a bean-shape plasma column spirals around a circular conductor, while the main toroidal field is generated by another system of circular coils (Fig. 7.5). A representative of this concept, TJ-II, has been built in Madrid and is now successfully in operation.

The interlinked coil system of Heliacs may not provide a direct reactor relevance but the TJ-II magnetic system provides a high degree of flexibility so that important equilibrium, stability and transport issues can be addressed.

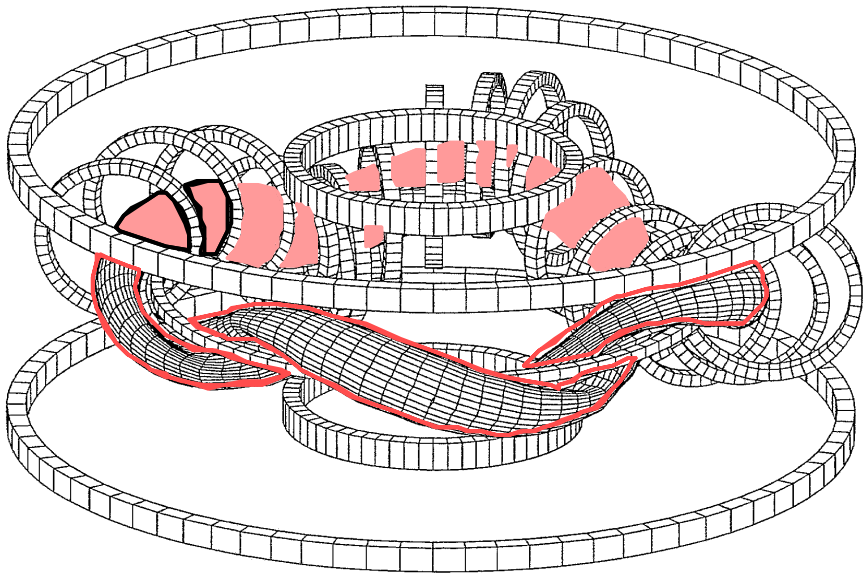

Fig. 7.5. Principle of a Heliac configuration.

7.3.4 Modular coil systems

The term modular stellarator refers to a generalized stellarator configuration of nested magnetic surfaces with multiple helicity achieved by a system of discrete coils which provides both toroidal and poloidal fields. Since there is no net toroidal current, no vertical-field coils are needed. A modular stellarator, therefore, has no toroidally continuous windings; the confinement coil system is modular. Furthermore, there is no force directed inwardly towards the minor axis. Thus the support structure can be located outside and on the sides of the coils. In classical stellarators and torsatrons, the windings providing the rotational transform are toroidal helices. These helical lines are shown in Fig. 7.6 in the unfolded θ-z plane, where z is the distance (or toroidal angle) along the toroidal direction. Let us consider a case where the currents in the helical windings and in the TF-coils are equal. Segmentation of the TF-coils and the helical windings and joining theses segments in a fashion as shown in Fig. 7.6 (b) yields non-planar and poloidally closed coils, which generate the same magnetic field as the original system. Since finite-size coils with small bending radii are not feasible, a smooth approximation to these modular coils is more favorable for practical application. The principle is shown in Fig. 7.7.

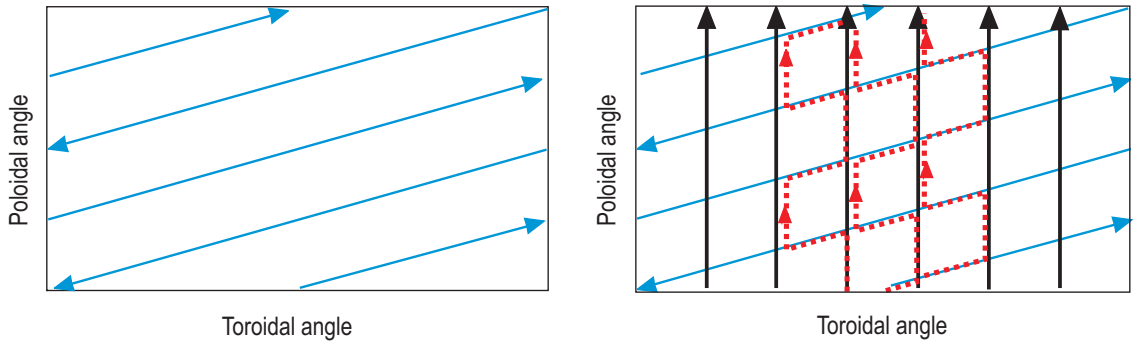

Fig. 7.6. **(a)** Helical windings on a toroidal surface. **(b)** Superposition of toroidal field coils (vertical arrows) and helical windings. The meander-like coils (dotted line) are equivalent to the system of TF-coils and helical windings.

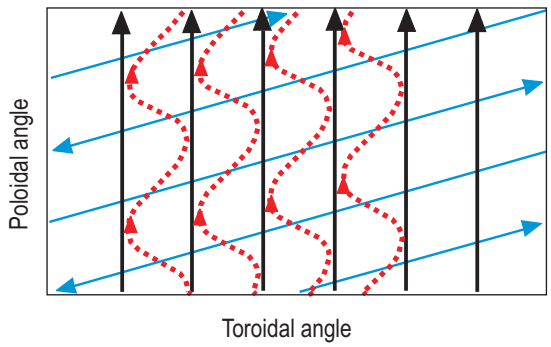

Fig. 7.7. Modular coils mapped into the θ-φ-plane. This system approximates the superposition of TF-coils and helical windings displayed in Fig. 7.6.

The idea of modular coils [72Wob] results from the fact that any toroidal vacuum field in a domain Ω and tangential to the surface $\delta\Omega$ can be produced by a current sheath on this surface. Discretizing this current sheath and thus forming current lines yields a set of modular and poloidally closed coils, which reproduce the magnetic field in the domain Ω to high accuracy. In a next step analytic winding laws were used to model these twisted coils and to generate the desired magnetic field and the rotational transform by a proper arrangement of these coils. In the Wendelstein 7-AS stellarator (Garching) [90Sap] and the IMS device (University of Wisconsin) [81And] this concept has been realized. A major step forward was provided by the idea of P. Merkel [87Mer] to calculate the system of surface currents on a second torus

$\delta\Omega_e$ surrounding $\delta\Omega$ such that the vacuum field produced by these surface currents is tangential to the given surface $\delta\Omega$ ($B_n = 0$ on $\delta\Omega$).

In the straight helically invariant stellarator described above the modular coils can be computed analytically. We consider the current sheath on the cylinder $r = a$. A sum in Bessel functions $I_n(nkr)$ describes the magnetic potential Φ_i inside the cylinder, in the outside region a similar expansion of the potential Φ_e in terms of the modified Bessel functions $K_n(nkr)$ can be given. On the cylinder $r = a$, the contour lines $\delta\Phi = \Phi_i - \Phi_e = \text{const.}$ are the current lines, which produce the given field of the potential Φ_i. Since the potentials Φ_i, Φ_e are single-valued – there is no net current in z-direction – the current lines are closed lines around the cylinder. Without the helical components we get the circular coils, which produce the main field $B_0 \boldsymbol{e}_z$. The generalization of this method to an arbitrary toroidal surface is the basis of Merkel's procedure.

The method to calculate the coil system after the magnetic field has been specified offers the chance to optimize the magnetic field first according to criteria of optimum plasma performance [87Nue] and then to compute the coil system after this procedure has come to a satisfying result. Along this line the advanced stellarator [83Bro] has been developed. In Wendelstein 7-AS (Fig. 7.8) this concept has been utilized to replace the helical windings of the previous experiment Wendelstein 7-A and to make use of the optimized magnetic field of an advanced stellarator. The concept of modular coils and the principle of optimization have been combined in the Wendelstein 7-X device [90Bei] (Fig. 7.9), which will demonstrate the reactor capability of the advanced stellarator line.

7.4 Physics basis of the stellarator reactor

7.4.1 Requirements on reactor physics

The requirements on the physics of a stellarator reactor are mainly determined by economic aspects and the limitations of the technical components.

- The fusion power output should be in the range of 3000…3500 MW, which at a given magnetic field of about 5 T leads to a plasma beta of 4…5 %. In this regime the plasma should be in a stable and well-centered equilibrium without violent transient phenomena.
- Energy losses should be small enough so that ignition and self-sustained burn is possible; plasma density and energy confinement time must satisfy the Lawson criterion $n\tau_E > 2 \times 10^{20}\ \mathrm{m^{-3}s}$. Losses of α-particles must be sufficiently small so that the internal heating power is not reduced and the wall load by highly energetic α-particles is kept at a tolerable level. Slowing down time of 3.5 MeV α-particles is of the order of 0.1 s, for this reason, highly energetic α-particles must be well confined at least for 0.1 s.
- The magnetic field is limited by the maximum magnetic field on the superconducting coils, which is 11 T in case of NbTi superconductors. For the reason of plasma confinement and stability limits a higher magnetic field is desirable, however this would imply to use NbSn superconductors or other advanced concepts. The mechanical load on the coils and the support structure grows quadratically with the magnetic field; in view of the complex structure of the coil system in stellarators – either the continuous coil system or the modular coil system – stresses and strains in the coils should be kept at tolerable values, also for this reason the magnetic field should be as small as possible.
- Radiation losses in the reactor plasma should be kept as small as possible. Bremsstrahlung and cyclotron emission are unavoidable, both grow with electron temperature, and for this reason the temperature at the operational point should be kept in the range from 12 to 20 keV. In view of the envisaged plasma beta this goal requires a plasma density in the range of $1\ldots3 \times 10^{20}\ \mathrm{m^{-3}}$.
- Stellarator experiments show that a density limit exists which results from the competing effects of impurity radiation, plasma transport and plasma heating. Therefore, good control of impurity influx and the efficiency of the divertor is an important requirement to the reactor plasma.
- There should be some means to control and to vary the power output of the stellarator reactor. Furthermore, full control of the start-up phase and the ramp-down is required.

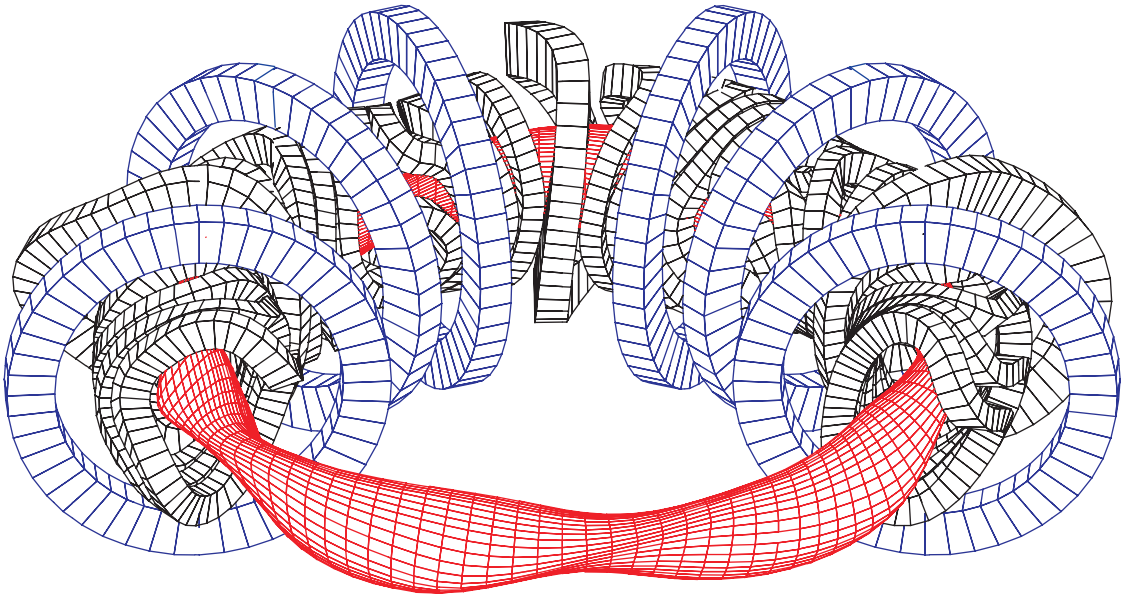

Fig. 7.8. Modular stellarator Wendelstein 7-AS. The standard magnetic field is generated by the modular coils alone. For experimental flexibility planar coils are superimposed to allow for variation of the rotational transform.

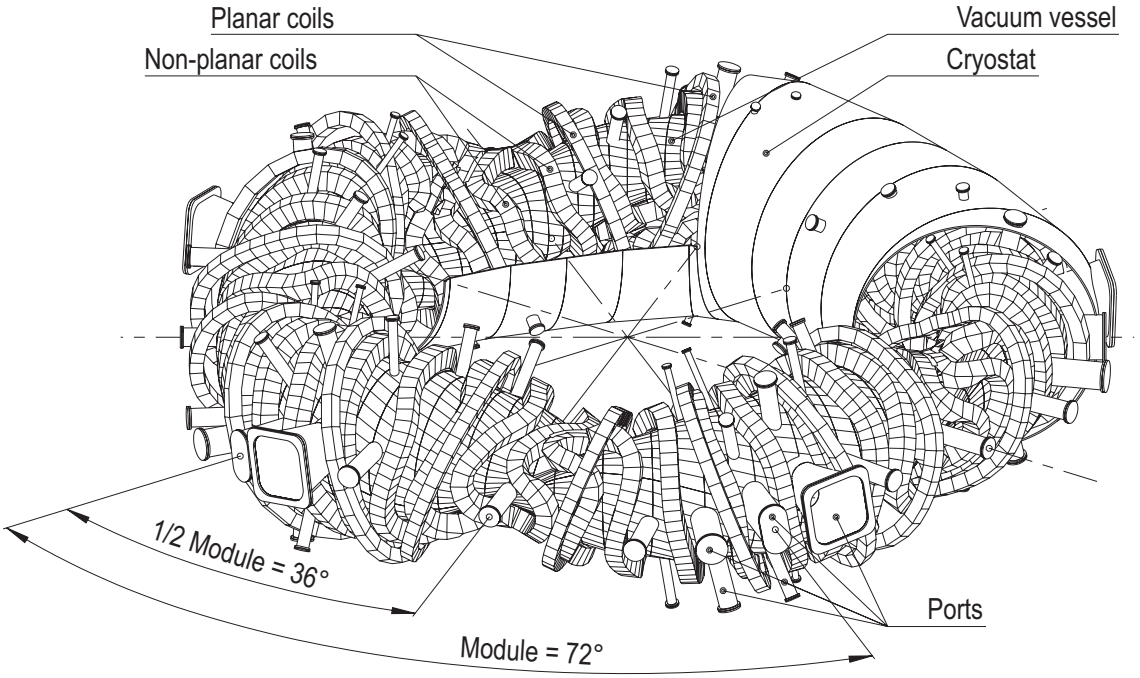

Fig. 7.9. Advanced stellarator Wendelstein 7-X (major radius 5.5 m, average plasma radius 0.5 m, magnetic field 3 T). The superimposed planar coils are required to improve experimental flexibility. The standard field is generated by the modular coils alone.

7.4.2 Plasma equilibrium

The model commonly used to describe equilibrium in stellarator configurations is the one-fluid model of ideal magneto-hydrodynamics. The gradient of a scalar pressure, ∇p, and the force $\boldsymbol{j} \times \boldsymbol{B}$ balance each other: $\boldsymbol{j} \times \boldsymbol{B} = \nabla p$, where $\nabla \cdot \boldsymbol{B} = 0$ and $\boldsymbol{j} = \nabla \times \boldsymbol{B}$. In systems with symmetries like axi-symmetric tokamaks or helically symmetric linear stellarators, these equations can be reduced to a two-dimensional quasi-linear elliptic equation, the Schlüter-Grad-Shafranov equation. In a 3-dimensional equilibrium, however, no such equation exists. L. Spitzer [58Spi] proposed an iterative scheme to solve the system. In this scheme a sequence $\boldsymbol{B}_\mathrm{n}$ of magnetic fields is constructed, which are assumed to converge towards a self-consistent equilibrium. This sequence is computed by $0 = \nabla p_\mathrm{n} + \boldsymbol{j}_{\mathrm{n}+1} \times \boldsymbol{B}_\mathrm{n}$, $\mu_0 \boldsymbol{j}_{\mathrm{n}+1} = \nabla \times \boldsymbol{B}_{\mathrm{n}+1}$. However, as pointed out by A. Boozer [84Boo], magnetic surfaces can be destroyed, even if the procedure begins with a set of nested surfaces. Numerical codes following this line have been developed by A. Reiman and H. Greenside [86Rei] and J. Kißlinger, H. Wobig [85Kis]. As shown by M. Kruskal and R. Kulsrud [58Kru], the force balance $\boldsymbol{j} \times \boldsymbol{B} = \nabla p$ can be derived from a variation principle which makes the positive functional

$$U = \iiint \left(\frac{B^2}{2\mu_0} + \frac{p}{\gamma - 1} \right) \mathrm{d}^3 \boldsymbol{x} \tag{7.1}$$

stationary (γ denotes the adiabatic coefficient). The constraints of this procedure follow from the conservation of fluxes during plasma motion. These constraints also avoid the problem of rational surfaces and the break-up into islands. Several numerical codes have been developed in the past to calculate equilibria by minimizing the functional U. Using the VMEC code [90Hir], J. Nührenberg and R. Zille have computed MHD-equilibria of advanced stellarators [86Nue]. The optimization criteria listed in the introduction have been included in this procedure to shape the plasma boundary in an appropriate way. A guideline to find the shape of toroidally optimized configurations is the result of the HERA code [81Gru] which computes helically invariant equilibria with an MHD-stability limit of $\langle\beta\rangle = 30$ %.

The Shafranov shift of magnetic surfaces is a characteristic feature of toroidal equilibria, with rising plasma pressure the inner surfaces are shifted radially outwards. In Wendelstein 7-AS this shift was measured and compared with theoretical predictions, as shown in Fig. 7.10. The Shafranov shift is clearly seen and reproduced in the equilibrium calculation. The reduction of the Pfirsch-Schlüter currents $\langle j_\parallel \rangle$ in W7-AS can directly be measured via the associated dipole field or indirectly via the measured Shafranov shift. Also data from the classical $l = 2$ stellarator, W7-A, are shown. The improvement observed and the good agreement with equilibrium calculations confirms the concept behind the optimization.

A series of equilibria of the Helias reactor has been computed using the NEMEC code and the MFBE code [99Str1]. The MFBE code allows one to compute the magnetic field outside the last magnetic surfaces, which is the indispensable basis of the divertor design. The magnetic surfaces of the vacuum field are shifted slightly to the inside by an appropriate vertical field, which has been built into the modular coils. The reason is the requirement to center the plasma column in the finite beta state at $\langle\beta\rangle = 4 \ldots 5$ % with respect to the first wall. This would lead to equal neutron wall-loading at the inboard and the outboard side. Although the plasma equilibrium in the Helias configuration has been optimized, the residual Shafranov shift can grow to 0.5 m.

The structure of the magnetic field and the islands outside the last closed magnetic surface (LCMS) change with rising plasma pressure. The five islands at the plasma boundary are envisaged for divertor action and for this reason it is desirable that the structure is nearly invariant to changes of the plasma pressure. In the Helias reactor case the islands grow with plasma beta, but the position of the O-point changes only by a small amount. In view of the envisaged divertor action of the islands this is a very desirable property. Self-consistent computation of a stellarator equilibria with magnetic islands is still an issue. The problem is that islands can exist on every spatial scale, which conflicts with the limited spatial resolution of numerical codes. The HINT code developed by Hayashi et al. [89Har] delivers some examples showing the complex structure of islands in a torsatron configuration.

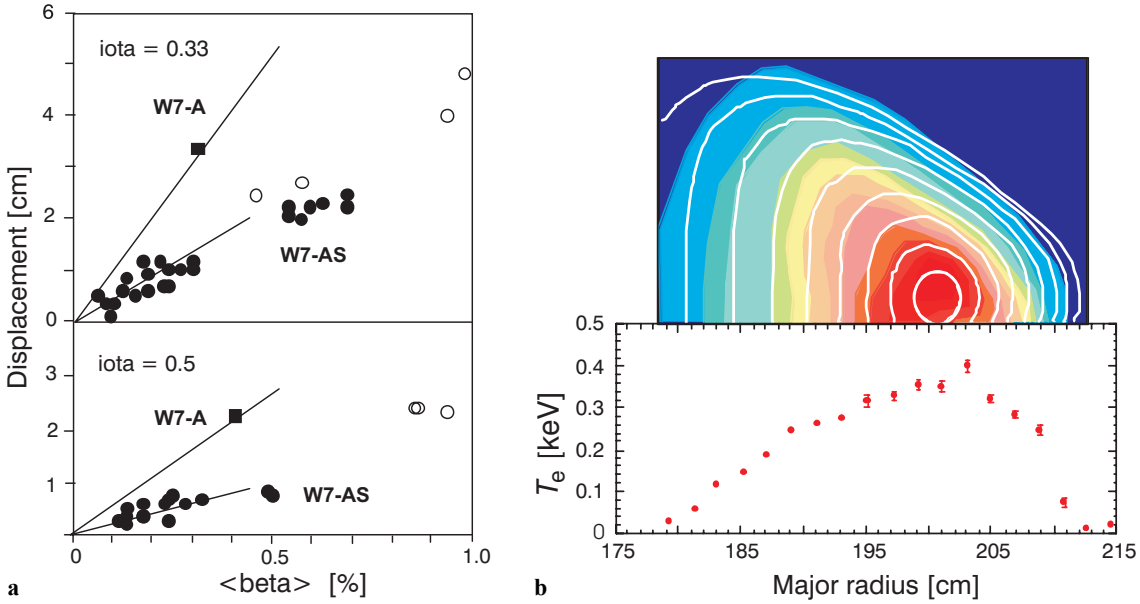

Fig. 7.10. **(a)** Shafranov shift of W7-AS (deduced from X-ray measurements) versus $\langle\beta\rangle$ for two ι-values (ι denotes the rotational transform of the field lines); the solid and open circles denote measurements at 2.5 T and 1.25 T, respectively. The squares are results from W7-A. The lines are the expected relations for the classical and partly optimized concepts. **(b)** Iso-contour diagram of the SX-emission of a high-β equilibrium of W7-AS, the calculated flux surfaces and the electron temperature profile of a $\langle\beta\rangle \approx 1.8$ % equilibrium.

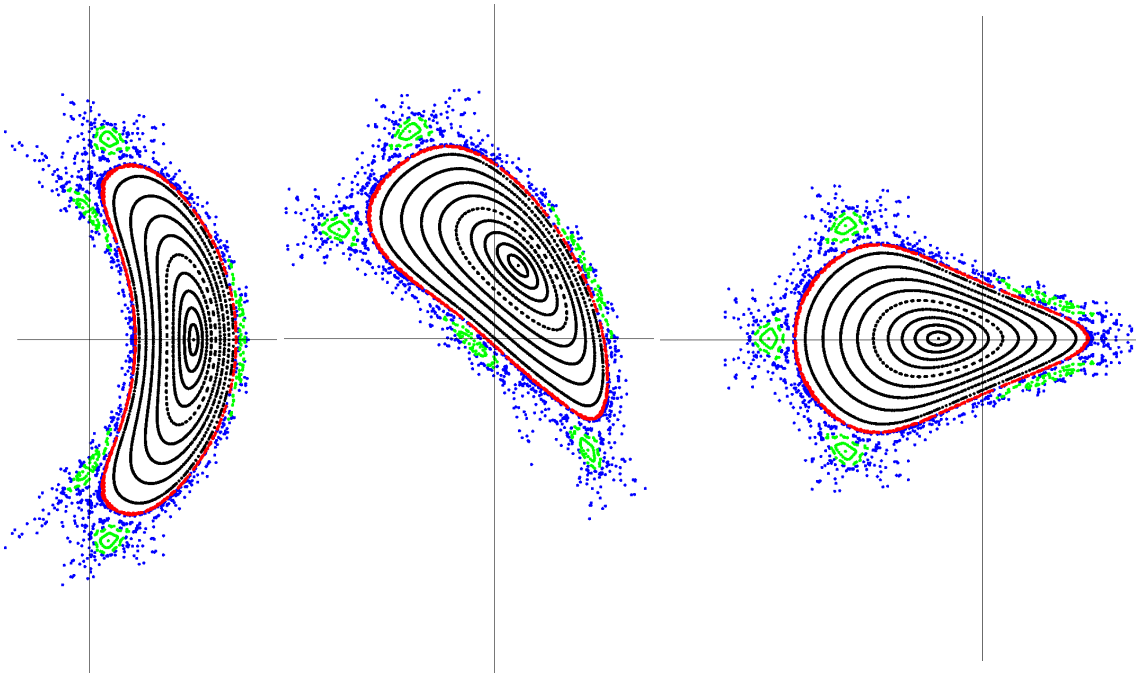

Fig. 7.11. Poincaré plot of magnetic surfaces of the Helias reactor HSR22 at $\langle\beta\rangle = 4$ % [89Har].

7.4.3 The role of Pfirsch-Schlüter currents

A key role in stellarator equilibria is played by the Pfirsch-Schlüter (P.S.) currents, which are closely connected to the Shafranov shift and to the radial drift of particles. In a toroidal equilibrium the plasma currcnt $\boldsymbol{j}$, which is needed to satisfy the equilibrium condition $\boldsymbol{j} \times \boldsymbol{B} = \nabla p$, usually is decomposed as a diamagnetic current $\boldsymbol{j}_\perp = \boldsymbol{B} \times \nabla p / B^2$ and a parallel current $\boldsymbol{j}_\parallel$. The first to compute these currents were D. Pfirsch and A. Schlüter [62Pfi], who found the approximation

$$j_\parallel = \frac{2 j_\perp}{\iota} \cos\theta \tag{7.2}$$

in an axisymmetric magnetic field $\boldsymbol{B}$, where ι is the rotational transform of the field lines and θ is the poloidal angle. This approximation has been made for stellarators without net toroidal current and large aspect ratio.

The parallel current density is closely related to the geometry of the magnetic field lines. The condition $\nabla \cdot \boldsymbol{e}_\mathrm{p} = 0$ yields a magnetic differential equation for the function $\lambda = (\boldsymbol{e}_\mathrm{p} \cdot \boldsymbol{B}) / B^2$.

$$\boldsymbol{B} \cdot \nabla \lambda = 2 \frac{|\nabla \psi|}{B} \kappa_\mathrm{g} \,, \tag{7.3}$$

where κ_g is the geodesic curvature of the field lines. If the geodesic curvature of field lines is small the plasma current flows nearly perpendicular to the magnetic field lines. The plasma currents grow with plasma pressure and so does the Shafranov shift. A large reduction of the parallel current has been reached in the Wendelstein 7-X configuration, however, extrapolating this to reactor size shows a maximum Shafranov shift of about 0.5 m.

In a general toroidal equilibrium the description of the plasma currents conveniently starts from the Hamada coordinate system (φ, θ are toroidal and poloidal coordinates, respectively, and s is the volume of the magnetic surface, the Jacobian of the coordinate system is 1) of a general toroidal equilibrium. In this coordinate system the magnetic field is given by $\boldsymbol{B} = \psi'(s)\boldsymbol{e}_\mathrm{t} + \chi'(s)\boldsymbol{e}_\mathrm{p}$ and the current density by $\boldsymbol{j} = I'(s)\boldsymbol{e}_\mathrm{t} + J'(s)\boldsymbol{e}_\mathrm{p}$, where $\boldsymbol{e}_\mathrm{p} = \nabla\varphi \times \nabla s$ and $\boldsymbol{e}_\mathrm{t} = \nabla s \times \nabla\theta$ are the poloidal and toroidal base vectors on the magnetic surface, ψ and χ are the toroidal and poloidal magnetic fluxes, I and J the toroidal and poloidal currents, respectively. The coordinate lines $\varphi =$ const. are poloidally closed and the lines $\theta =$ const. are toroidally closed. In general these base vectors are not orthogonal ($\boldsymbol{e}_\mathrm{p} \cdot \boldsymbol{e}_\mathrm{t} \neq 0$). The parallel component of the current density in (7.1) does not affect the force balance, however, these parallel currents generate a poloidal dipole field, which leads to a radial shift of the plasma column, the Shafranov shift. If $\nabla \cdot j_\perp$ were zero, there would be no parallel current and zero or only small Shafranov shift. Thus, designing magnetic field configurations where $\nabla \cdot j_\perp$ is as small as possible is the basic optimization criterion of the advanced stellarator.

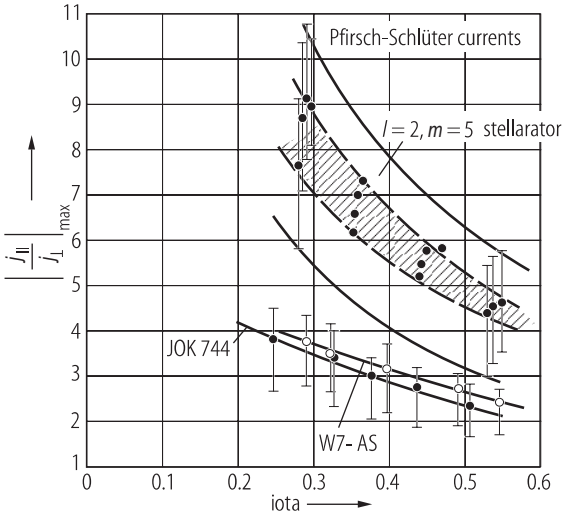

Fig. 7.12. Ratio beween parallel current density and diamagnetic current density versus iota. JOK 744 is a configuration similar to W7-AS.

7.4.4 Classical diffusion and Pfirsch-Schlüter currents

Although stellarator experiments show that in some regions diffusion is larger than classical or neoclassical it is useful to analyze these phenomena in detail, since classical diffusion is the unavoidable minimum of plasma losses. Plasma resistivity is the origin of classical and Pfirsch-Schlüter diffusion. Therefore the starting point is Ohm's law, $-\nabla\Phi + \boldsymbol{v}\times\boldsymbol{B} = \eta\boldsymbol{j}$, so that from the diffusion velocity results

$$\boldsymbol{v}(x) = -\eta\frac{\nabla p}{B^2} + \frac{\mathbf{B}\times\nabla\Phi}{B^2}\,. \tag{7.4}$$

The first term in this equation is the classical diffusion velocity, and the second is the convective velocity giving rise to Pfirsch-Schlüter diffusion. The electric field in this velocity is calculated from the parallel component of Ohm's law, $-\nabla\Phi\cdot\boldsymbol{B} = \eta\boldsymbol{j}\cdot\boldsymbol{B}$, and it is obvious from this relation that in stellarator configurations with small parallel currents this electric field is also small and consequently the Pfirsch-Schlüter diffusion is small, too. The word diffusion in "Pfirsch-Schlüter diffusion" is misleading because it is not a local diffusion process where the flow vector $\boldsymbol{v}$ is proportional to a local gradient as it is in the case of classical diffusion. The convective velocity in (7.4) is proportional to $\nabla\Phi$, and this gradient is not related locally to the pressure gradient. However, the integrated net flux is of interest and this flux can be correlated to the pressure gradient $p'(s)$. The total diffusive flux Γ through a magnetic surface is given by

$$-(\psi'(s))^2\,\Gamma = \eta\left\langle \boldsymbol{e}_\mathrm{p}\cdot\boldsymbol{e}_\mathrm{p}\right\rangle p'(s)\,, \tag{7.5}$$

where the brackets < > denote the average over a magnetic surface. Classical and Pfirsch-Schlüter diffusion can be characterized by the diffusion coefficient

$$D = \frac{n\eta}{(\psi'(s))^2}\left\langle \boldsymbol{e}_\mathrm{p}\cdot\boldsymbol{e}_\mathrm{p}\right\rangle. \tag{7.6}$$

Approximating the cross section of magnetic surfaces by circles leads to the equation

$$\left\langle \boldsymbol{e}_\mathrm{p}\cdot\boldsymbol{e}_\mathrm{p}\right\rangle \approx \rho^2\left(1+\frac{2}{\iota^2}\right), \tag{7.7}$$

where ρ is the averaged plasma radius. This classical and Pfirsch-Schlüter diffusion only occurs if the plasma is collision-dominated and if there are no turbulent losses. In a fusion plasma the collisional approximation is no longer valid and the mean free path is much larger than the size of the plasma. In that case details of particle orbits leading to neoclassical diffusion will determine the confinement.

7.4.5 Stability of stellarator equilibria

In order to get a fusion power output which is large enough for economic reasons the plasma pressure and the pressure gradient must be as high as possible. Limits to the plasma pressure are set be the onset of MHD-instabilities, which either prevent a further increase of the pressure or – in the worst case – lead to a rapid termination of the discharge. Experiments so far do not show that the latter scenario is a realistic one, however, stellarator experiments have not yet reached the beta values envisaged in a reactor, e.g. 4…5 %.

Unavoidable driving terms in a toroidal plasma are the pressure gradient together with the unfavorable or convex curvature of magnetic field lines. In a stellarator without toroidal net current the energy source behind tearing modes and disruptive instabilities, which are the plague of the tokamak concept, is absent.

Although local unfavorable curvature cannot be avoided, a surface-veraged favorable curvature or a magnetic well can be achieved. Magnetic shear is also a stabilizing agent in a stellarator, however, the stabilizing effect is annihilated by plasma resistivity. Analytically the stability criterion against MHD-perturbation with small wavelengths is the resistive interchange criterion,

$$[\psi']^4 < \frac{B^2}{|\nabla s|^2} p' \frac{\psi''(s)}{\psi'(s)} + (p')^2 \left\langle \frac{\boldsymbol{e}_\mathrm{p} \cdot \boldsymbol{e}_\mathrm{p}}{|\nabla s|^2} \right\rangle < 0, \tag{7.8}$$

which shows that the magnetic well – described by the term $\psi''(s) / \psi'(s)$ – should be sufficiently large to make the critical pressure gradient large enough. Ballooning modes are localized to regions of unfavorable curvature and they mainly define the beta-limit of a stellarator.

Numerical investigations of the MHD-stability of a Helias reactor have shown stability up to an averaged beta of 4 %. This result was found by local ballooning mode analysis and by global mode analysis with the CAS3D code [93Nue]. Both methods yield instability at $<\beta> = 5$ %. Interpolating the results of CAS3D results in a stability limit of 4.2 % [99Str2]. Low-order rational magnetic surfaces, which do not exist in the vacuum field, can exist in the finite beta plasma. This concerns the 5/6 resonance, which appears for $<\beta> \geq 4$ %. Since at this point a global mode is expected, the occurrence of $\iota(0) = 5/6$ is used as a definition of the MHD-stability limit. The magnetic well deepens with rising beta, which is a decisive feature in providing MHD-stability.

7.4.6 Particle orbits in stellarators

The basic problem of particle confinement in stellarators is the lack of continuous symmetry, which destroys absolute confinement of particles. Absolute confinement means that for $t \to \infty$ the particles stay in a finite domain. The inhomogeneity of the magnetic field leads to a drift of the gyrating particles and this radial drift cannot be averaged to zero for all particles. Especially highly energetic α-particles whose orbits are barely affected by radial electric fields and collisions need to be confined for at least one slowing down time which is about 0.1 s in a stellarator reactor. Particle orbits in a fusion plasma are usually described in guiding center approximation with the magnetic moment as an adiabatic invariant. Because of this invariance the mirror force affects the parallel motion of the guiding center and the particles can be trapped in local mirrors. In particular these localized particles experience a non-zero average radial drift and can be rapidly lost towards the plasma boundary. The local drift of a guiding center is

$$\boldsymbol{v}_\mathrm{D} = \frac{\boldsymbol{E} \times \boldsymbol{B}}{B^2} + \left(v_\parallel^2 + \frac{v_\perp^2}{2} \right) \frac{\boldsymbol{B} \times \nabla B}{\Omega B^2} \; ; \; \Omega = \frac{eB}{m}, \tag{7.9}$$

where m is the mass of the particle, e denotes its charge, and Ω is the gyro frequency. The normal component of the drift velocity on magnetic surfaces is the origin of neoclassical losses, and therefore minimizing this component is the method to reduce these losses. This radial component is related to the geodesic curvature of the field lines,

$$\boldsymbol{v}_\mathrm{D} \cdot \frac{\nabla s}{|\nabla s|} = \left(v_\parallel^2 + \frac{v_\perp^2}{2} \right) \frac{\kappa_\mathrm{g}}{\Omega}, \tag{7.10}$$

where the radial electric drift does not contribute to radial losses. Thus, reduction of geodesic curvature will affect the orbits of all classes of particles. The drift surfaces of circulating particles will stay closer to magnetic surfaces, and trapped particles localized in a magnetic mirror will also be better confined than in a classical stellarator. The bounce-averaged radial drift of trapped particles – using (7.9) – can be written as:

$$\oint \boldsymbol{v}_\mathrm{D} \cdot \nabla s \frac{\mathrm{d}l}{v_\parallel} = \frac{m}{e\psi'(s)} \oint \left(v_\parallel^2 + \frac{v_\perp^2}{2} \right) \boldsymbol{e}_\mathrm{p} \cdot \frac{\nabla B}{B} \frac{\mathrm{d}l}{v_\parallel}, \tag{7.11}$$

with l being the length along the field line. The recipe to improve confinement of trapped particle is to localize these particles in regions of small geodesic curvature or small poloidal variation of B. However, even if the radial drift of trapped particles is small, the poloidal drift of these particles should be sufficiently large to prevent large excursions from magnetic surfaces. If the poloidal drift is small or zero,

super-banana orbits occur and the orbits extend to the plasma edge. This effect is particularly important for α-particles in a stellarator reactor. Confinement of highly energetic α-particles in a Helias reactor depends on the poloidal magnetic drift, which increases with rising plasma pressure.

$$\left\langle \boldsymbol{v}_{\mathrm{D}} \cdot \boldsymbol{e}_{\mathrm{p}} \right\rangle = \oint \left(v_{\parallel}^2 + \frac{v_{\perp}^2}{2} \right) \left(\kappa_n + \boldsymbol{n} \cdot \frac{\nabla p}{B} \right) \frac{|\nabla \psi|}{\Omega B^2} \frac{\mathrm{d}l}{v_{\parallel}}, \tag{7.12}$$

where $\boldsymbol{n}$ is the normal vector on magnetic surfaces. The poloidal drift consists of two terms, the first one related to the normal curvature of field lines, κ_n, can change sign and thus leads to turning points of the poloidal drift. This is the origin of super-banana orbits. The second term increases with plasma pressure and leads to a unidirectional poloidal drift. As a result the recipe to improve the confinement of trapped particles is to localize them in the region of small geodesic and normal curvature. The poloidal magnetic drift of finite-beta plasma also improves the confinement of trapped particles. In particular, the confinement of high-energy α-particles depends on this effect. Numerical computations in the Helias configuration based on the second adiabatic invariant have verified these conclusions. Torsatron configurations with low aspect ratio have also been optimized by analyzing the J*-contours of trapped particles [98Spo].

7.4.7 Neoclassical transport in stellarators

The synergetic effect of trapped particle orbits and Coulomb collisions can lead to strong radial losses of these particles, which has two consequences. Firstly, confinement of thermal particles may become so low that ignition is not possible and secondly, highly energetic α-particles can escape towards the wall on a time scale short compared with the slowing-down time and thus diminishing the internal heating of the fusion plasma. Neoclassical transport in stellarator configurations has been studied by various methods:

- Monte Carlo techniques,
- analytical solution of the bounce-averaged drift kinetic equation,
- numerical solution of the drift-kinetic equation (DKES code).

The Monte Carlo code calculates transport coefficients by convoluting mono-energetic results with a Maxwellian distribution and appropriate weighting factors. The same technique is used in the DKES code [86Hir]. For neoclassical ion transport, details of the configuration are less important than the presence of a radial electric field Φ', which in the case of $e\Phi' / kT' \approx 1$ reduces the diffusion coefficient well below the plateau level. Therefore, electron behavior is of great importance since it is less affected by the electric field (electrons largely being in the $1/\nu$ regime, where ν is the collision frequency). The main features of neoclasssical transport in stellarators are illustrated in Fig. 7.13.

For conventional stellarators, the magnetic field is described by

$$B = B_0 \left(1 - \varepsilon_{\mathrm{t}} \cos\theta + \varepsilon_{\mathrm{h}} \cos\left(l\theta - m\varphi \right) \right), \tag{7.13}$$

where $\varepsilon_{\mathrm{t}} = r / R$ is the inverse aspect ratio, ε_{h} denotes the coefficient of the helical field, and (θ, φ) are magnetic coordinates which are designed to render field lines on magnetic surfaces straight. The function $B(s, \theta, \varphi)$ fully determines the particle orbits. The diffusion coefficient in the $1/\nu$ regime is

$$D_{1/\nu} = \text{const.} \cdot \varepsilon_{\mathrm{h}}^{3/2} \frac{\varepsilon_{\mathrm{t}}^2}{\nu}, \tag{7.14}$$

In Helias configurations, $D_{1/\nu}$ may be expressed in a similar manner with the helical ripple ε_{h} replaced by an "equivalent ripple" $\varepsilon_{\mathrm{eff}}$, which is found to be ≈ 0.01…0.02 for the Helias configurations under consideration. This result has been confirmed by each of the different methods listed above and demonstrates the strong reduction of neoclassical transport in Helias configurations compared with non-optimized stellarators, where this value may be as large as 0.1 or more.

Particles trapped in modular ripple wells do not experience a reduction in their radial drift; these losses can only be kept small by a small modular ripple. Extensive studies using the bounce-averaged drift-kinetic equation [88Bei] were undertaken to calculate these losses, resulting in the conclusion that at least 10 coils per field period are required if modular ripple losses are to remain smaller than helical ripple losses for every flux surface in the plasma cross section [89Bei].

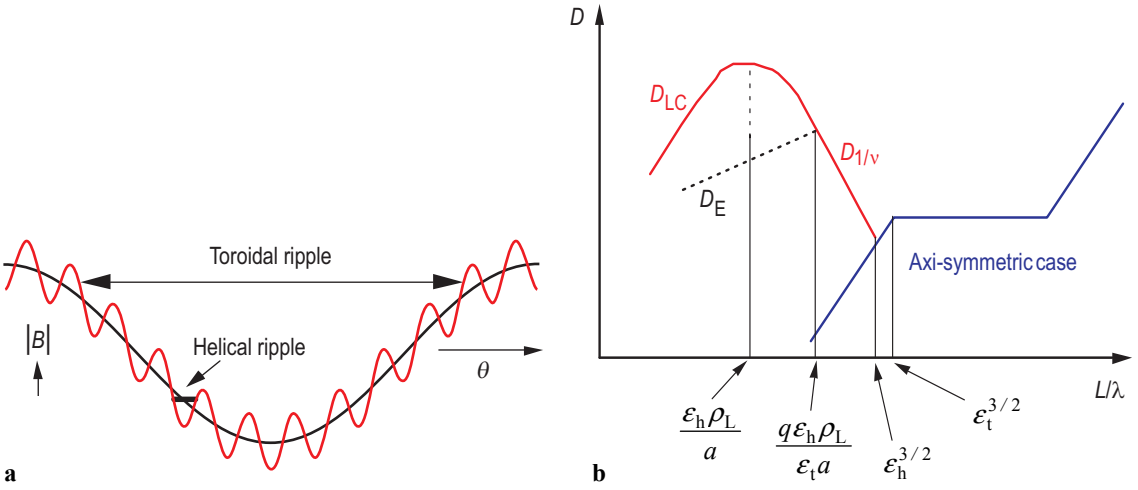

Fig. 7.13. **(a)** Variation of $|\boldsymbol{B}|$ along a field line for a poloidal circumference (toroidal and helical component). On the abscissa, the poloidal angle, θ, is drawn. **(b)** Scheme of neoclassical transport for the axi-symmetric case and the stellarator case, showing the diffusion coefficient, D, versus the normalized inverse mean free path, L/λ.

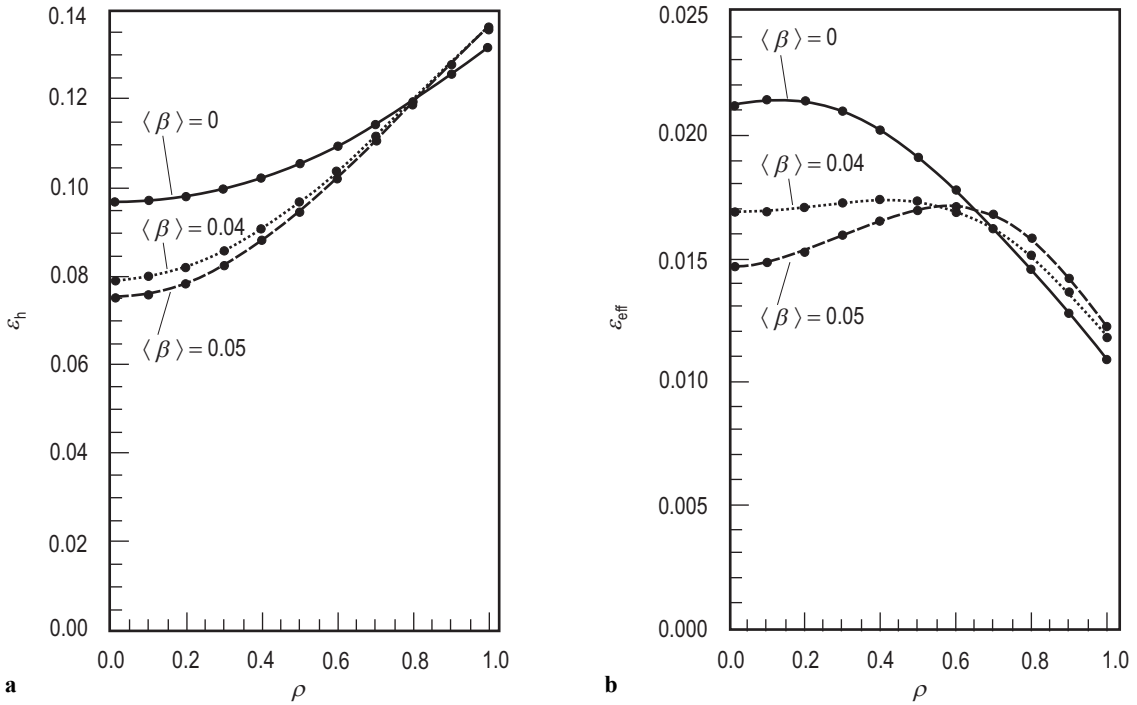

Fig. 7.14. Neoclassical transport in HSR. **(a)** Geometrical ripple. **(b)** Effective helical ripple. Average beta between 0 and 5 % (numerical results by C.D. Beidler).

7.4.8 The bootstrap current

Another neoclassical effect is the bootstrap current, which is a toroidal current driven by the anisotropic pressure of the plasma. Since this anisotropy grows with the mean free path, this current may become large in reactor-relevant regimes. The bootstrap current leads to a shift of ι with increasing plasma pressure. It is mainly this shift of ι across low-order rational surfaces, associated with deteriorated confinement, that requires the selection of advanced stellarator configurations with a greatly reduced bootstrap current. The bootstrap current can be minimized by a proper choice of $B(s, \theta, \varphi)$ in conjunction with other principles of optimization. A reduction of a factor of 20 could be achieved, which implies that the bootstrap current is only 5 % of the bootstrap current in an equivalent axi-symmetric device ($\varepsilon_h = 0$).

The theory of the bootstrap current could be confirmed by experiments in Wendelstein 7-AS, thus providing confidence that extrapolations to Wendelstein 7-X or a stellarator reactor are credible.

Maximum values of the bootstrap current up to 10 kA are measured in W7-AS. It has to be noted that W7-AS is not designed for low bootstrap current. Because of the dominance of the toroidal curvature in the W7-AS field design the bootstrap current increases the rotational transform as it is the case in tokamaks. Figure 7.15 plots the measured versus the calculated bootstrap current. Good agreement is found which supports the expectations of a low bootstrap current for Wendelstein 7-X.

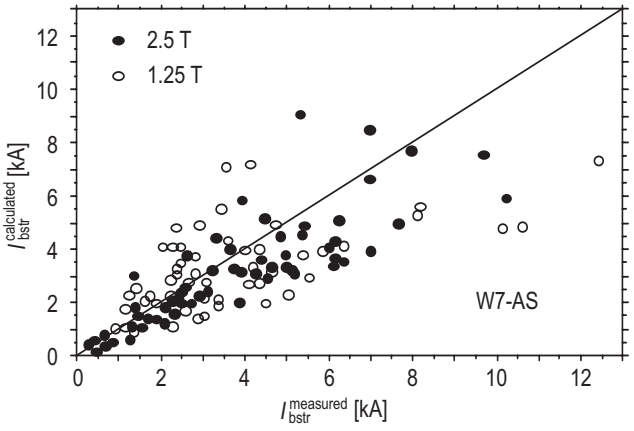

Fig. 7.15. The bootstrap current measured in W7-AS is compared with the calculated values. Results from two field values, 1.25 T and 2.5 T, are shown.

7.4.9 Principles of optimization in stellarators

At the IPP-Garching, the effort to extrapolate the stellarator to a viable reactor has led to the Helias concept [86Nue], where by proper choice of the magnetic field configuration the currents flowing in the plasma can be reduced to a low level where the currents parallel to the magnetic field (Pfirsch-Schlüter currents) are smaller than the diamagnetic currents. As a consequence the radial shift of the plasma column with rising plasma pressure – the Shafranov shift – is strongly reduced and the MHD-stability limit is raised to values around $\langle\beta\rangle \approx 5$ %. In essence the conditions for an optimized reactor configuration are

- Good magnetic surfaces of the vacuum field without major resonances, islands and stochastic regions in the bulk plasma. Islands or stochasticity in the boundary region may be utilized for divertor action.
- Low Shafranov shift and a stiff equilibrium configuration up to $\langle\beta\rangle = 5$ %. The rotational transform should depend only weakly on the plasma pressure.
- MHD-stability up to $\langle\beta\rangle \approx 5$ %. Sufficiently small neoclassical plasma losses so that the ignition condition is satisfied.
- Sufficiently small bootstrap currents so that the magnetic field is not modified by this effect.
- Good confinement of α-particles.
- Good technical feasibility of the coil system and sufficiently large space between coils and plasma for blanket and shield.

To fulfill one or two of these requirements is not difficult, the important result, however, is that all conditions can be met simultaneously in one configuration. The geometrical shape of the Helias configuration, the number of periods, rotational transform etc. are consequences of these optimization criteria. The method used to find an optimized Helias configuration differs essentially from the standard method, which starts from a given coil system and calculates the plasma behavior afterwards. In the Helias approach a fixed plasma boundary $d\Omega$ is the starting point for computing the plasma equilibrium inside this boundary and the coil system outside. The plasma equilibrium in the domain Ω is calculated using fixed boundary codes [86Hir]. The shape of $d\Omega$ and the pressure profile determine all properties of the equilibrium; by continuous variation of the boundary, which is described by 10 parameters, the required optimum can be found.

With respect to particle confinement, quasi-helical [88Nue] or quasi-axisymmetric systems are highly optimized. In these configurations trapped particles stay on magnetic surfaces, which in particular for α-particles is a favorable feature.

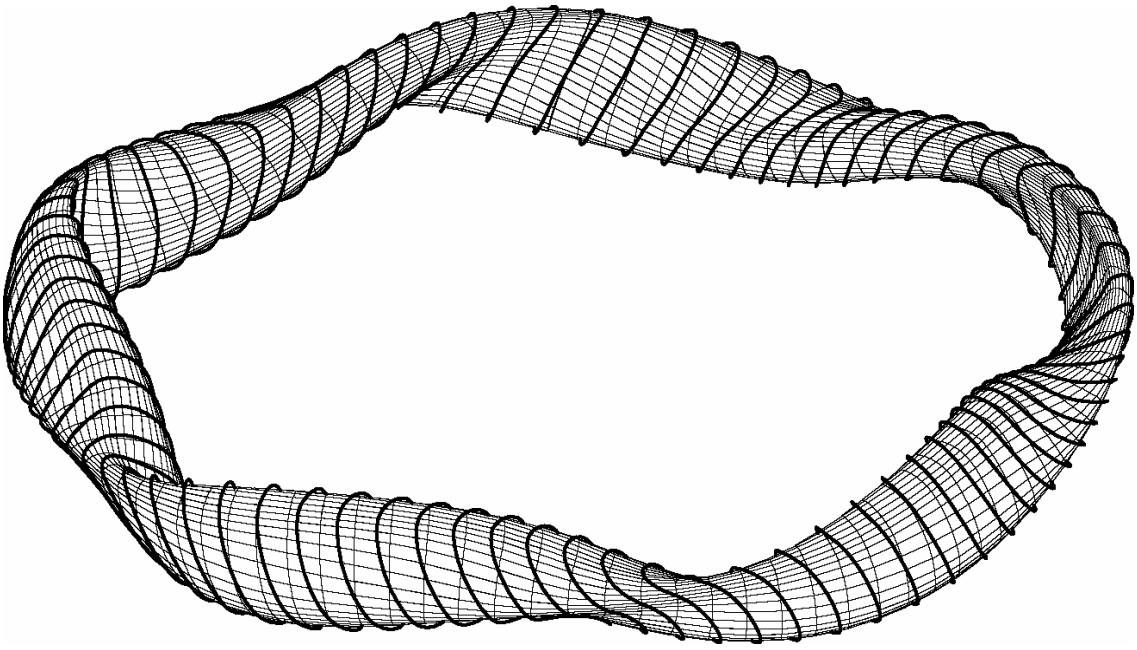

Fig. 7.16. Magnetic surface of the advanced stellarator Wendelstein 7-X. Solid black lines are the current lines on the magnetic surface. In some regions the current lines are nearly perpendicular to the field lines.

7.4.10 Alpha-particle confinement

Good confinement of highly energetic α-particles is a necessary condition for self-sustaining operation of the fusion process in a stellarator reactor. In this context the following problems are of importance:

- Sufficient confinement of trapped α-particles,
- a small number of particles trapped in the modular ripple,
- anomalous losses of α-particles by plasma oscillations.

Numerical investigations of α-particle orbits in a Helias reactor have shown that the losses of α-particles trapped in a modular ripple can be sufficiently reduced in case of ten modular coils per period. A smaller number of coils would raise the ripple-induced losses appreciably. The majority of trapped α-particles is trapped in the basic field period. As already shown by W. Lotz et al. [92Lot], poloidal magnetic drift in the finite beta equilibrium improves the confinement of these particles such that only a small

fraction of trapped particles is lost in a time shorter than one slowing down time. In the present reactor configuration, however, this number is still too large; more than 10 % of the heating power is lost by poorly confined α-particles. Thus, further fine-tuning of the magnetic field is necessary to improve the classical confinement of α-particles further.

The quasi-helical configurations and quasi-axisymmetric configurations are an important development in stellarator optimization [88Nue]. In a quasi-helical stellarator, the field varies (in magnetic coordinates) in the form $B = B(s, l\theta - n\varphi)$, which leads to closed drift surfaces of all particles. Being like a tokamak from the single particle point of view, a quasi-helical stellarator has a tokamak-like bootstrap current. Therefore, a careful compromise must be found in extrapolating this concept towards a reactor.

Even after the classical losses of α-particles have been minimized to an acceptable level another source of losses may arise due to resonant interaction with electric and magnetic oscillations in the plasma. At the beta limit, excitation of Alfvén waves or drift Alfvén waves is to be expected and, if some characteristic frequencies of the particle orbits match the frequencies of the waves, resonant losses may occur [99Wob1]. Solving the guiding center equations α-particle orbits under the influence of time-dependent and time-independent oscillations have also been studied by A.A. Shishkin et al. [98Shi]. In all these studies the amplitude of the oscillations has been treated as a free parameter, which indicates the need for a self-consistent solution of this issue. According to the present knowledge the prompt losses of highly energetic α-particles can be reduced to a few percent, which is not an issue for the power balance of the plasma, but the consequences of the lost α-particles impinging on the wall is still an unexplored region.

7.4.11 Distortion of the magnetic field

The external magnetic field generated by the coil system must satisfy certain requirements with respect to resistance against field errors, which imposes some constraints on the accuracy of the coils and the alignment of the coils. This problem has already been faced in present stellarator experiments and it was possible to keep the relative construction error below 10^{-3}. In stellarators the use of ferromagnetic material has always been a matter of concern, since the vacuum field of the coils may be distorted and the magnetic surfaces can be destroyed. In particular, this issue arises in a Helias reactor where ferritic-martensitic steel is utilized as structural material. Because of its low activation properties this material is highly favored in modern fusion reactor concepts. The strong magnetic field of a fusion reactor drives the steel into saturation and the effective permeability is in the range of 1.3…1.5. The distortion of the magnetic field of the coils by ferritic inserts with these properties has been studied analytically in a straight and helically invariant $l = 2$ stellarator and numerically in a Helias reactor [99Har]. It has been found that the destruction of magnetic surfaces does not occur if the 5-fold symmetry of the configuration is conserved. A small reduction of the rotational transform by 1…2 % is not a serious effect and can easily be compensated. These computations, however, only refer to the distortion of the vacuum magnetic field by ferritic matter; how much the self-consistent plasma equilibrium will by modified by the ferritic matter in the surrounding blanket is still an open problem.

7.4.12 The divertor in the stellarator reactor

The purpose of a divertor in a fusion reactor is to control a large fraction of 600 MW α-heating on its way onto material target plates. The requirements are that the local power deposition must not be too large (≤ 5 MW/m^2) and that impurity ions released from the first wall and the target plates are confined in the divertor region. Under optimistic assumptions the impurity ions convert a large fraction of the α-heating power into radiation forming a radiative mantle or photosphere around the hot plasma core. The geometry of the divertor plasma is determined by the magnetic field in the boundary region. In torsatrons of LHD-type the helical divertor has as structure similar to the X-point divertor of tokamaks except for the helical geometry of the structure. In the Helias reactor magnetic islands provide the divertor action, where on the

backside of these islands target plates are located. At the plasma boundary of HSR a rational surface with $\iota = 1$ exists. Five islands exist on this surface which will be used as divertors. The plasma currents tend to modify these islands with rising beta, however it has been found that the position of the O-point is shifted only by a small amount. The increasing ergodization of the surfaces in the island region is not an obstacle to the envisaged divertor action; it may even help to divert the plasma flow. There is a strong similarity to the divertor of a tokamak, except for the helical structure of the X-point. Divertor target plates must follow the helical structure of the X-line. Inherently the structure of the divertor region is three-dimensional and requires a three-dimensional model to describe the plasma behavior in this region.

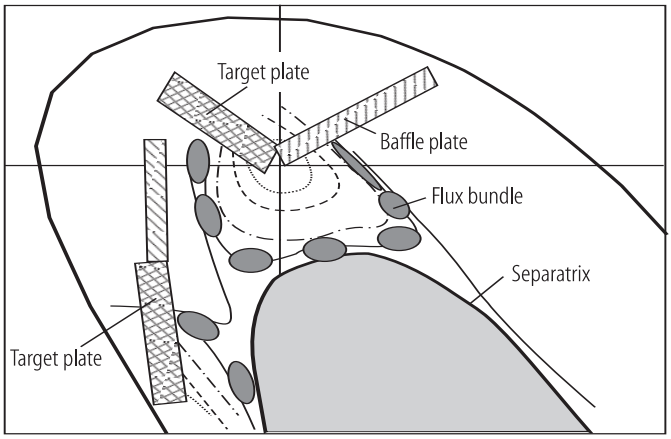

Fig. 7.17. Islands and divertor plates at $\iota = 1.0$ in the HSR magnetic field. Finite beta plasma at $<\beta> = 4$ %. Result of VMEC + MFBE.

Figure 7.17 shows that about three or four toroidal turns are needed before the field lines or the flux bundles, which begin close to the separatrix, arrive at the back of the islands. The connection length in this case is about 400 m. The modification of the magnetic structure in the divertor region with growing plasma pressure has some negative effects on the start-up phase or shutdown phase of the discharge, since fixed divertor target plates do not match all magnetic configurations. The technical layout of the divertor plates will be very similar to the design in Wendelstein 7-X. The goal is to design the divertor structure as an integrated part of the blanket segments, which will certainly facilitate the maintenance process. The specific power load onto the divertor plates depends on the transport mechanism in the divertor region and the radiative layer.

7.4.13 Anomalous transport in stellarator reactors

Plasma experiments in stellarators show a strong evidence of anomalous transport and of energy confinement, which is lower than predicted by classical or neoclassical transport theory. Since a good understanding of the physics of enhanced transport processes is lacking so far, the confinement properties are described by an empirical scaling law of the energy confinement time. This energy confinement time – the ratio between plasma energy content and net heating power – is modeled by a power law in terms of the plasma density, the heating power, magnetic field and some geometrical data of the device: major radius, plasma radius and rotational transform. Extrapolating these scaling laws to reactor conditions allows one to compute the confinement time of the reactor plasma and to check whether the ignition condition or for self-sustained burn are satisfied. Several scaling laws of energy confinement have been proposed. These are: the Lackner-Gottardi scaling (LGS) [90Lac], the gyro-Bohm (GRB) scaling and the LHD scaling (LHD). The international stellarator scaling (ISS95) [96Str] has been derived from a data base summarizing all existing stellarator experiments. These results are listed in Table 7.6 (ISS95 and ISS_{W7}). The scaling law ISS_{W7} is derived from Wendelstein 7-AS and Wendelstein 7-A data only. The general form of these scaling laws is a power law,

$$\tau_E = \text{const.}\, R^{a1} a^{a2} B^{a3} \langle n \rangle^{a4} P^{a5} \kappa^{a6} \iota^{a7} A^{a8}, \tag{7.15}$$

with major radius R, minor plasma radius a, magnetic field B, heating power P, elongation of magnetic surfaces κ (unity in stellarators), effective atomic mass A, line-averaged density $<n>$, and rotational transform ι.

The Helias reactor is an upgraded version of Wendelstein 7-X. It is more closely related to low-shear configurations such as Wendelstein 7-A and Wendelstein 7-AS than to high-shear devices. Therefore extrapolating confinement times on the basis of LGS or ISS_{W7} scaling may be the most relevant procedure to check the ignition capability of a Helias reactor.

Table 7.6. Coefficients of the empirical scaling laws.

Coefficient	LGS	ISS95	ISS_{W7}	LHD	GRB
const.	0.175	0.256	0.36	0.17	0.25
a5	–0.6	–0.59	–0.54	–0.58	–0.68
a1	1.0	0.65	0.74	0.75	0.6
a2	2.0	2.21	2.21	2.0	2.4
a3	0.8	0.83	0.73	0.84	0.8
a7	0.4	0.4	0.43	0.0	0.0
a4	0.6	0.51	0.5	0.69	0.6

There are two effects which can lead to a deterioration of these scaling laws of confinement times. One reason could be radiation losses of impurity ions, which accumulate in the plasma center and reduce the achievable plasma energy and the confinement time. This means that the confinement time is smaller and ignition is harder to achieve. The second effect is the onset of plasma instabilities at the beta-limit leading to an increase of radial transport and consequently to a reduction of the confinement time. If this occurs above the ignition point it may help to stop the thermal instability of the fusion plasma. If the onset of strong MHD-instabilities happens below the ignition point, it can prevent the ignition.

The scaling laws listed above are obtained under conditions of L-mode confinement in stellarators, and it will be shown below that this can be sufficient for ignition. H-mode confinement could also be achieved in stellarators as in tokamaks, however, improvement of confinement was only of the order of 30 %.

7.4.14 Empirical scaling laws and ignition

The general condition for self-sustained burn in a fusion reactor is that the product of plasma density and confinement time be large enough: $n\tau_E > 2 \times 10^{20}$ m^{-3}s. Since the confinement times in Table 7.6 grow with the plasma dimensions R and a and also with magnetic field and density, the ignition condition can always be meet if the plasma is large enough, the magnetic field large enough and the plasma density high enough. However, all these parameters are limited from above: the size must not be too large for economic reasons, the magnetic field should stay below a certain limit in order to comply with he requirements of superconducting coils, and the density is limited by radiative effects. Thus, in selecting the dimensions of a stellarator reactor a compromise among conflicting requirements must be made.

A rough survey over the ignition capability of a stellarator reactor can be obtained by modeling the anticipated plasma parameters and to check whether the required confinement is equal to or smaller than the confinement times resulting from the scaling laws described above. The required confinement time is defined by the plasma energy and the α-particle heating power reduced by the losses due to Bremsstrahlung $E/\tau_E = P_{\text{alpha}} - P_{\text{brems}}$. In order to allow for a self-sustained burn this confinement time must be shorter than or equal to the confinement times described above.

Since stability analysis predicts a beta-limit of 4.2 % in HSR22, the issue arises whether presently known scaling laws of energy confinement are compatible with the requirements of ignition. The ISS95-scaling [96Str] predicts a confinement time which is too low by at least a factor of two. Experiments in Wendelstein 7-AS and Wendelstein 7-A are also fitted well by the Lackner-Gottardi scaling, which – if

applied to the Helias reactor – meets the ignition condition [98Bei2]. This scaling, although it may not be the only one, is also supported by recent experiments in the LHD device [00Tak].

A consistent set of parameters of the fusion plasma, which fits to the requirements listed above, is given in Table 7.7.

The peak density in the Helias reactor is assumed to be as high as 3×10^{20} m^{-3}, which is comparable with the highest densities achieved in Wendelstein 7-AS. This allows one to operate the fusion plasma at low temperature (15 keV), while the fusion output is still sufficiently large.

The required energy confinement time is 1.6 s. The extrapolation of empirical confinement times shows that some of these do not meet the ignition condition. Predictions according to LHD-scaling or ISS95-scaling yield a confinement time which is too small, confinement times on the basis of LG-scaling or W7-scaling are sufficient. Confinement of thermal α-particles is a matter of concern. If the fraction of thermal α-particles is greater than 6…7 %, the dilution effect leads to an intolerable reduction of the fusion power.

Table 7.7. Parameters of a Helias reactor.

Major radius	22.00 m
Minor radius	1.800 m
Plasma volume	1407 m^3
Iota(a)	1.000
Equivalent current	3.498 MA
Magnetic field on axis	5 T
Maximum field on coils	10.00 T
Line averaged density	2.126×10^{20} m^{-3}
Electron density $n(0)$	3.040×10^{20} m^{-3}
Electron temperature $T(0)$	15.00 keV
Average electron temperature	4.965 keV
Beta(0)	15.67 %
Average beta	4.241 %
Fusion power	3000 MW

Table 7.8. **C**onfinement times and fusion power.

Plasma energy	8.036×10^2 MJ
Energy confinement time	1.622 s
α-particle confinement time	1.337×10^1 s
Energy confinement time (LHD)	5.095×10^{-1} s
Energy confinement time (LGS)	1.648 s
Energy confinement time (W7)	2.092 s
Energy confinement time (ISS)	9.614×10^{-1} s
Bremsstrahlung loss	1.003×10^2 MW
Cyclotron radiation (0)	1.843×10^4 W/m^3
Cyclotron radiation	4.264 MW
Fusion power	3.064×10^3 MW
Internal heating power	4.912×10^2 MW

7.5 Economic aspects of a stellarator reactor

In connection with the economic feasibility of stellarator reactors the following aspects are important and also provide some guidelines how to optimize stellarator reactor design.

- Feasibility and reliability of the coil system. The coil system is the most expensive single component of the reactor core, and therefore requires a careful choice of the superconductor taking account of the required magnetic field and the complex structure of the coil system with its inhomogeneous distribution of forces.
- Blanket systems and tritium cycle. The choice of the blanket has strong influence on the nuclear safety of the reactor, on the amount and composition of nuclear waste and on the availability of the reactor.
- Thermal cycle and efficiency of plant. The choice of the blanket fixes the temperature of the cooling medium and thus the efficiency of the thermal cycle.
- Fuel cycle. The fuel cycle is the place where the tritium is being recovered and reprocessed, a special difference between stellarators and tokamaks does not exist.
- Safety and environmental considerations. Many safety aspects are common to stellarators and tokamaks, therefore the comprehensive assessment of safety issues in tokamaks also applies to stellarators. In the following, some differences between the two concepts will be pointed out.
- Availability of plant. Scheduled and unscheduled shutdown times define the availability of the plant. Fault conditions and the issue of blanket replacement are the decisive problems in stellarator reactors.
- Cost considerations. Cost estimates following the ARIES tokamak procedure have been made in the MHH study.

7.5.1 Wall loading

First wall and other plasma facing components are subject to strong loading by neutrons, charged particles, neutral particles and electromagnetic radiation. The largest fraction stems from 14 MeV neutrons, however, in stellarators the average neutron wall load is rather low, the reason being the large area of the first wall, which keeps the average power load in the order of 1 MW/m^2. In poloidal and toroidal direction the power load is inhomogeneous with a peaking factor 1.7…1.8 (see Table 7.9). Charged particles and their energy are deposited on divertor target plates while charge exchanged neutrals deposit energy onto the first wall, in particular in those regions where the distance between plasma and first wall is smallest.

Table 7.9. Power flow onto first wall.

		MHH	HSR22
Neutron power	[MW]	1380	2400
Area of first wall	[m^2]	1171	2600
Average neutron power load	[MW/m^2]	1.18	0.92
Peaking factor		1.79	1.7
Peak power loading	[MW/m^2]	2.11	1.56
α-particle heating power	[MW]	346	600
Radiation (50 % of P_{alpha})	[MW]	173	300
Radiative wall loading	[MW/m^2]	0.15	0.12
Power to target plates	[MW]	173	300
Max. power density on target plates	[MW/m^2]	5	5
Wetted area on target plates	[m^2]	35	60

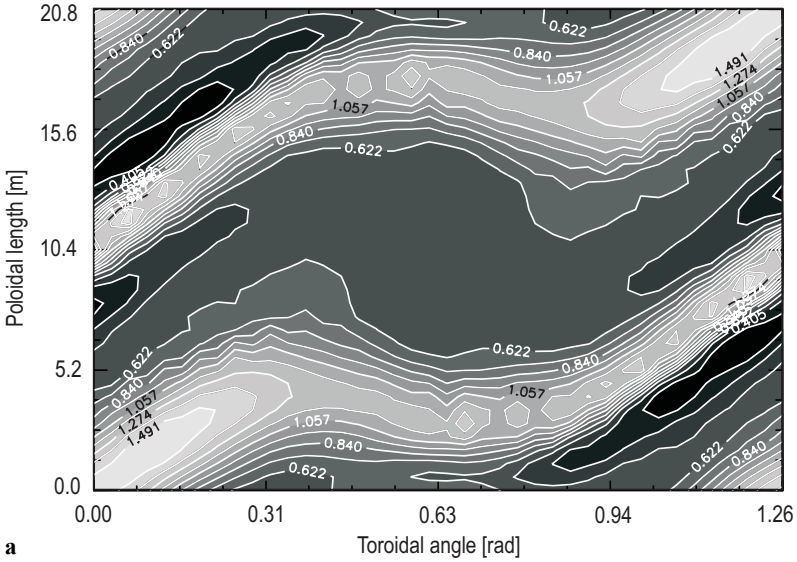

a

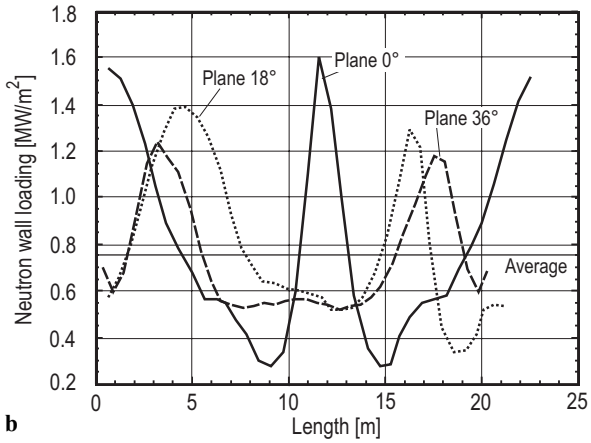

b

Fig. 7.18. **(a)** Contour lines of neutron wall load in HSR22. Abscissa: toroidal angle, one field period of 72°. Ordinate: Poloidal direction, length in m. **(b)** Poloidal distribution of neutron wall loading in HSR (3200 m^2 area). Plane 0° means toroidal angle $\varphi = 0°$, corresponding to the left or right margin of (a). Plane 36° means $\varphi = 36°$, corresponding to the center of (a).

The maximum power load by electromagnetic radiation occurs if the plasma is detached and all α-particle heating power is converted to electromagnetic radiation. If the plasma is not detached, a rough assume yields that 50 % of the α-power is radiated. Bremsstrahlung is the minimum radiation power in any fusion reactor, it is peaked in the plasma center and therefore nearly equally distributed around the torus as the neutron power. Losses by cyclotron radiation are rather low in stellarator reactors, if the temperature can be kept below 20 keV.

The large size of HSR22 provides a large area of the first wall and a slightly smaller average neutron power loading than in the more compact MHH reactor. The specific radiative wall load is about the same in both reactor concepts. Power load onto the divertor target plates is about 50 % of the total α-power and is nearly twice as large in HSR22 as in MHH; however, in view of the larger area off target plates in HSR22 the specific load onto the target plates is about the same in both cases. The maximum allowable thermal power on target plates in fusion devices is about 5 MW/m^2, which leads to a minimum wetted area of 60 m^2 (HSR) and 35 m^2 (MHH), respectively.

The lifetime of first wall and blanket depends on the neutron fluence and on the limits of the structural material. The MHH study assumed a limit of 200 dpa of the Vanadium alloys, corresponding to a blanket lifetime of 11 a. The end-of-life fluence is 16.4 MWa/m^2 (peak) and an average fluence is about 9.1 MWa/m^2. Given these optimistic assumptions the blanket lifetime in HSR22 (also equipped with V-alloys) would be 13.5 a. Here it is assumed that the availability of the reactor is 76 %. More conservative studies of blanket performance [99Mal] assume a maximum average fluence of 6 MWa/m^2, leading to 9 a lifetime in HSR22.

7.5.2 Blanket systems in stellarator reactors

As in any toroidal fusion device the purpose of the blanket is to provide sufficient breeding of tritium and to shield the superconducting coils against neutrons. Since atomic processes determine the size of the blanket, its radial width is an absolute figure and any fusion device has to provide enough space to accommodate a blanket with about 1.3 m radial build. In contrast to tokamaks the stellarator, however, requires a 3-dimensional design of the blanket, which must conform to the 3-dimensional shape of the plasma. Blanket segments must be small enough to be replaceable through portholes, therefore a stellarator needs a large variety of different modules, which in case of the Helias reactor HSR22 is 250 comprising 25 different shapes. The various blanket concepts, which have been studied for tokamak reactors [98Yam], are also suited in stellarators. The MHH design favors a self-cooled lithium blanket, while in the torsatron reactor FFHR molten salt FLIBE ($LiF\text{-}BeF_2$) has been selected [98Yam]. Either a solid breeder blanket (HCPB [94Don]) or a liquid LiPb blanket with additional cooling [95Mal] are the options in the Helias reactor HSR22 [99Wob2], as presented in Table 7.10.

The most attractive option for HSR22 is the self-cooled LiPb blanket with additional helium cooling. This concept provides high efficiency of the thermal cycle and avoids the hazards associated with water cooling or the use of large amounts of beryllium. The large weight of the LiPb is a drawback, but the liquid breeder material is reusable and hence not considered as nuclear waste. This also holds for beryllium, which must be reprocessed and separated from tritium.

The torsatron reactor FFHR provides good access between coils to the blanket underneath, however, because of the narrow spacing of 1 m between plasma and coils, the blanket must be carefully designed and the shielding of coils is still an issue. Liquid Li, as proposed in the MHH-study, provides good breeding ratio, however, because of its chemical hazards it is not a favorable candidate.

Table 7.10. Blanket options in the modular reactor HSR22.

Helium-cooled solid breeder		LiPb blanket	
Number of segments	280	Number of segments	280
Length (inboard/outboard)	10 m	Av. Length of segment	10 m
Total mass of breeder	201 t	Volume of segment	8 m^3
Total mass of beryllium	2951 t	Mass of breeder	60.8 t
Mass of structure	10.5 t	Mass of structure	9.4 t
Total mass of breeder zone	2951 t	Weight of segment	70.2 t
Weight per segment	10.5 t	Void	5 %
Mass of shield/manifolds	4131 t	Total mass	19656 t
Total (blanket/shield)	7082 t	Mass of Pb-17Li	17024 t
		Structure	2632 t
Coolant	He	Coolant	H_20
Temperature (inlet/outlet)	250/450 °C	Temperature (inlet/outlet)	265/325 °C
		Self-cooled + He	/600 °C

7.5.3 Thermal cycle

The thermal cycle in a reactor comprises the power flow from the reactor to the convertor and the various loops of the recycling power. As an example we consider a stellarator reactor with $P_{fus} = 3000$ MW thermal fusion power. Basically the power flow in stellarator and tokamak reactor is the same with the exception of the recycling power needed for current drive in tokamaks. Most of the thermal power is carried by neutrons to the blanket ($P_n = 2400$ MW) and after having passed the heat exchange system the thermal power is converted to electricity, P_e (efficiency η_c). In the blanket, nuclear processes enhance the thermal power described by a blanket multiplication factor η_b, which is about 1.2…1.4 depending on the blanket

design. The α-heating power (P_α = 600 MW) finally ends on the divertor target plates by charged particles and on the first wall in form of bremsstrahlung or – if a detached plasma can be maintained – as impurity radiation. The power onto the first wall is recovered in the cooling circuit and added to the blanket power. Let be η_w the fraction of α-power dumped on the first wall and $1 - \eta_w$ the fraction to the divertor, then the total thermal power is

$$P_{th} = \eta_b P_n + \eta_w P_a + \eta_d (1 - \eta_w) P_a , \tag{7.16}$$

where η_d is the efficiency of the divertor cooling. To improve the overall efficiency of the power plant the cooling power of the divertor plates must be included in the total thermal power. To avoid two separate cooling circuits the blanket and the divertor use the same inlet temperatures.

As in tokamak reactors the stellarator reactor needs a certain fraction of recycling power to feed all consumers of electricity in the power plant. The main part goes into the cooling system of the coils and into the pumps of the blanket cooling system. In the MHH power plant study a power of 11 MW was estimated for the cryo-plant. This power is dumped to the environment as low-grade heat, however the power to the cooling pumps can be recovered with a certain efficiency and reused in the primary coolant loop. Re-circulating power, which is used in vacuum pumps, tritium recovery system, pellet injection system, control systems etc. is certainly not recoverable and will be dumped as thermal waste. In the SPPS study the fraction of re-circulating power was estimated to be 5 % of the total electric power.

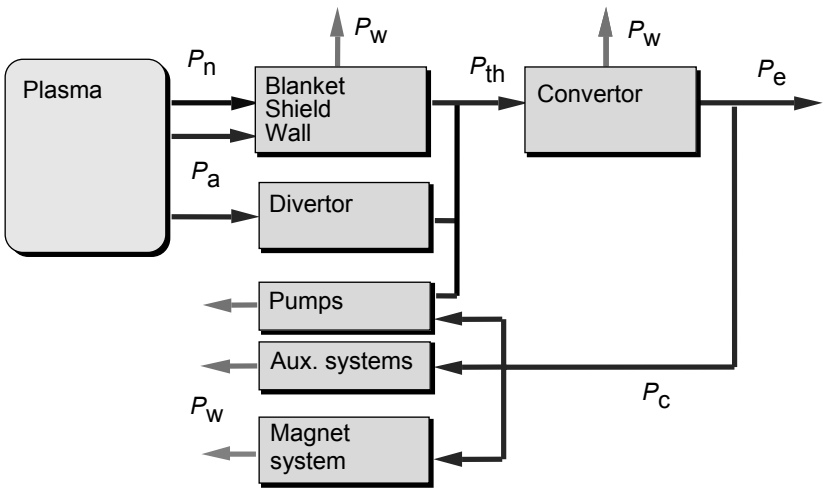

Fig. 7.19. Power flow diagram in a stellarator reactor.

The electricity output depends crucially on the thermal conversion efficiency of the convertor and on the outlet temperature of the cooling system. The MHH power plant study (SPPS [97UCS]) assumes an outlet temperature of 610 °C, which allows a conversion efficiency of 46 %. This efficiency can be reached with the advanced Rankine cycle as proposed in the ARIES tokamak reactor studies [93Naj] (see Table 7.11). The temperature in the thermal cycle is limited by the allowable temperatures of the structural material. The choice in the SPPS study is vanadium alloy (V5Cr5Ti) where the limits are 650…750 °C.

The thermal power balance and the efficiency of the plant depend strongly on the choice of the breeder and the structural material. A helium-cooled liquid lead blanket was proposed in the ASRA-6C study [87Boe2] leading to an overall efficiency of 42.7 %. To achieve a sufficient breeding ratio a large amount of beryllium had to be added in the blanket, which is a disadvantage from the point of view of safety. With respect to blanket, structural material and cooling cycle there is no difference between the modular ASRA6 stellarator and a modern Helias stellarator. Blanket options, which have been designed for tokamak reactors, can also be used in stellarators; however, the three-dimensional shape of the plasma requires also a three-dimensional shape of the blanket. Lowest efficiency is achieved with a water-cooled LiPb-blanket. Table 7.12 lists the data of a Helias reactor for various blanket concepts.

Table 7.11. Summary of the thermal cycle in the MHH reactor.

Fusion power	1730 MW
α-power	346 MW
Neutron power	1380 MW
Multiplication factor	1.4
Thermal power	2280 MW
Conversion efficiency	0.46
Gross electric power	1050 MW
Re-circulating power fraction	0.052
Net electric power	1000 MW
Net plant efficiency	0.44

Table 7.12. Power flow in a Helias reactor.

Fusion power	3000 MW		
α-power	600 MW		
Neutron power	2400 MW		
		Self-cooled LiPb blanket	Water-cooled LiPb blanket
Multiplication factor		1.3	1.2
Thermal power	[MW]	3720	3480
Conversion efficiency		0.46	0.35
Gross electric power	[MW]	1711	1218
Recycling power	[MW]	95	95
Net electric power	[MW]	1625	1123
Thermal waste	[MW]	2008	2262

7.5.4 Safety of stellarator reactors

Safety issues of a tokamak reactor have been extensively studied by J. Raeder et al. [95Rae]. Many results of this study can be extrapolated to stellarator reactors since the total number of neutrons produced per second, which is 10^{21} in a 3000 MW reactor, is a function of the envisaged fusion power alone. This implies that the integrated effects of the neutrons in the structure, and thus the amount of nuclear waste, is the same in both reactor types. On the other hand, stellarator and tokamak reactors differ in size, coil system and size of the blanket, which has some consequences for the safety issues. Tritium inventory and possible mobilization of tritium by accidents is a main issue in any fusion reactor. First investigations of failure modes in a Helias reactor have been undertaken in connection with the SEAFP-99 study [99Por].

7.5.4.1 Energy reservoir

In the Helias reactor HSR22 the overall stored magnetic energy of the coil system is 100 GJ. For comparison: The magnetic energy of the SEAFP device is 180 GJ in 16 TF coils. Furthermore, the disruption as a major initiator of a quench does not exist in stellarators. A quench is the biggest accident of the coil system of the superconductor, which must be mitigated by a quench detection system and the conversion of the magnetic energy into dump resistors. An upgraded version of the detection system of Wendelstein 7-X has been designed for this purpose [98Wie].

The energy in the plasma, which can be released into instabilities, consists of several contributions:

- thermal energy 760 MJ,
- magnetic energy of diamagnetic currents 700 MJ,
- magnetic energy of Pfirsch-Schlüter currents 6.5 MJ.

There is no induced toroidal current or a bootstrap current. The design of the magnetic field includes zero bootstrap current as one of the design criteria. Such a case will be verified and tested in Wendelstein 7-X. The absence of a toroidal current eliminates the energy reservoir, which can drive tearing modes and disruptive instabilities. This conclusion also holds for neoclassical tearing modes, which in tokamaks degrade the confinement. In a stellarator without toroidal current only pressure-gradient-driven MHD-instabilities are possible. Approaching the critical pressure gradient would result in a soft onset of unstable modes and increasing radial plasma losses. There are no experimental or theoretical arguments so far, which predict a violent collapse at the beta limit. In conclusion, any collapse of the plasma energy occurs on the time scale of the energy confinement time, which is of the order of 1.5 s.

7.5.4.2 Tritium inventory

The fuel cycle of a fusion reactor consists of two loops, one is the tritium recovery system which extracts the tritium from the blanket, and the other one is the exhaust system. By far the largest amount of tritium is circulating in the exhaust system. The tritium inventory in the exhaust is determined by the throughput of tritium and the amount of dust deposited in the pumping ducts and in the reprocessing units. Since in HSR dust is released only by normal operation and not by disruptive events, it is expected that the amount of dust can be kept smaller than in an equivalent tokamak. The number of tritons in the plasma volume is 1.22×10^{23}. If the particle confinement time is $5 \times \tau_E = 7.5$ s ($\tau_E = 1.5$ s) this requires a refueling rate of 1.63×10^{22} tritons/s, which is 293 g/h or 7.04 kg/d. This implies that 7 kg tritium per day must be extracted from the exhaust, reprocessed and refuelled into the plasma. However, with respect to safety the instantaneous inventory of tritium is relevant. As in any 3000 MW fusion reactor the tritium burn-up per day is 470 g, therefore in steady state about 520 g (breeding rate 1.1) must be recovered per day from the breeding blanket. There is no specific difference between tokamaks and stellarators, therefore the extensive studies on this issue performed in the NET, DEMO, SEAFP, ITER design also apply to stellarators. However, because of the larger volume of the breeding blanket the amount of tritium produced per volume element is smaller, so that a larger amount of coolant material, either helium or liquid lithium/lead, must be processed.

Tritium implantation into the first wall and the blanket structure sums up to a larger amount than in a smaller tokamak blanket. The area of the first wall in HSR is about 2400 m^2 (without divertor target plates and baffle plates). With tungsten as armor material the extrapolation from SEAFP (1400 m^2) yields an implanted amount of tritium of 86 g. If we apply this enhancement factor to the other components, then we get the following result: PFC armor (tungsten) 86 g, first wall (martensitic steel) 51 g, blanket structure 34 g, breeder 34 g, coolant system 102 g, water 68 g. The tritium inventory in the plasma facing components and the breeding blanket is proportional to the area of the first wall and to the volume of the blanket resulting is a larger inventory than in a tokamak with comparable fusion output.

7.5.4.3 Decay heat

Decay heat of activated material is a potential hazard in case of loss of coolant. This issue has been considered in the SEAFP report, where it is shown that the decay heat is proportional to the neutron flux. Since the neutron flux in average is 0.92 MW/m^2, this implies that the decay heat in the Helias reactor is smaller than in the SEAFP device. Accordingly the temperature rise will be smaller than expected in SEAFP. The overall decay heat integrated over the blanket volume, however, is probably the same as in a tokamak device since the integrated neutron flux is the same.

7.5.5 Balance of mass and cost analysis

Stellarators and tokamaks differ in the reactor core, which contributes one third of the total costs of the power plant. For this reason a large difference in cost cannot be expected and a careful study of all advantages and disadvantages is needed for a credible comparison of the two reactor candidates. To reduce the capital cost there is a strong incentive to make the reactor core as small as possible. In this respect the large aspect ratio of stellarators is a drawback leading to a relatively large size of the coil system and the blanket. On the other hand, access from outside and inside, availability and running costs of the reactor will be positively affected. The MHH study came to the conclusion that the total capital costs of both systems are about equal. Hender et al. [96Hen] obtained the same result in an earlier study.

The coil system is the most expensive single item of the reactor core, and here some differences among the stellarator concepts and in comparison to tokamaks will be expected. Continuous coil systems require another manufacturing technique than modular coil systems. Furthermore, using NbTi or Nb_3Sn in the superconductor makes a large difference in price. Although a detailed cost analysis of modular Helias reactors has not yet been made, some cost-saving effects and trends can be pointed out. The magnetic field of the modular Helias reactor is kept at 5 T in the plasma and below 11 T on the coils, which allows one to utilize a NbTi superconductor instead of a more expensive Nb_3Sn superconductor. Another cost saving factor is to reduce the major radius of the reactor while keeping the plasma volume constant and the magnetic field at 5 T. The result of these efforts is a 4-period Helias reactor with 18 m major radius, HSR18 [00Kis]. This implies that the capital cost will be reduced by about 20 % in comparison to the reference reactor HSR22. On the other hand in a more compact device neutron wall loading will be larger and the lifetime of plasma facing components will be reduced. A comparison of both reactors is given in Table 7.13.

Table 7.13. Parameters of HSR22 and HSR18.

		HSR22	HSR18
Major radius	[m]	22	18
Average plasma radius	[m]	1.9	2.1
Plasma volume	[m^3]	1420	1420
Average aspect ratio		11	8.5
Iota		0.83/1.0	0.83/1.0
Magnetic field	[T]	5	5
Number of periods, coils		5, 50	4, 40
Average radius of coils	[m]	5.5	5.5
Weight of coil	[t]	94	94
Coil system	[t]	4700	3760
Mass of structure	[t]	7000	5000
Volume of cryostat	[m^3]	26530	21480

The coil system is enclosed by a cryostat with rectangular cross section the volume of which is smaller than the volume of the cryostat in the ITER FDR design.

Availability of the fusion reactor depends on scheduled and unscheduled downtimes. The failure probability of many reactor components is the same in stellarators and tokamaks, a difference, however, arises from the absence of some effects like disruptions and some components like current drive, which is not needed in stellarators. Scheduled outages due to maintenance and replacement of blanket modules require the same procedure in both concepts if maintenance is performed through portholes between coils. By parallel operation on all periods around the torus it is possible, in principle, to achieve the same downtime in small or large devices. In that case the relatively long lifetime of blanket and first wall raises the availability of the stellarator reactor compared to more compact devices with a smaller lifetime. Although an extensive and quantitative cost assessment of a stellarator reactor does not yet exist it can be concluded that stellarators are competitive candidates for a viable fusion reactor.

7.6 References for 7

54Spi Spitzer, L., Grove, D., Johnson, W., Tonks, L.,Westendorp, W.: Problems of the Stellarator as a Useful Power Source, USAEC Report NYO-6047 (1954).

58Joh Johnson, J.L., Oberman, C.R., Kularud, R.M., Frieman, E.A.: Phys. Fluids **1** (1958) 281.

58Kru Kruskal, M., Kulsrud, R.: Phys. Fluids **1** (1958).

58Spi Spitzer Jr., L.: The Stellarator Concept, Phys. Fluids **1** (1958), 253.

61Mil Mills, R.G.: Economic Prospects for Thermonuclear Reactors, Princeton Plasma Physics Laboratory report MATT-60 (February 1961).

62Mil Mills, R.G.: Engineering Aspects of Magnetohydrodynamics, Columbia University Press, NY, (1962) 514.

62Pfi Pfirsch, D., Schlüter, A.: MPI-Report PA/7/62 (1962).

66Pop Popov, S.N., Popryadukhin, A.P.: Soviet Physics – Tech. Phys. **11** (1966) 284.

69Gib Gibson, A.: Permissible Parameters for Economic Stellarator and Tokamak Reactors, Proc. BNES Nuclear Fusion Reactor Conf. at Culham Laboratory (September 1969) 233.

70Col Cole, H.C., Hill, J.W., Terry, M.J.: Plasma Heating by Neutral Injection in a Stellarator Reactor, Proc. 6th Symp. on Fusion Technol., Aachen, FRG, EURATOM report EUR 4593e (September 1970) 479.

70Gou Gourdon, C., Hubert, P., Marty, D.: Comptes rendus hebd. séances acad. sci. Paris, Vol. II, **271** (1970) 843.

71Gib Gibson, A., Hancox, R., Bickerton, R.J.: Economic Feasibility of Stellarator and Tokamak Fusion Reactors, Proc. 4th Inter. Conf. on Plasma Physics and Controlled Nuclear Fusion Research, IAEA-CN-28/K-4, III (June 17-23, 1971) 375.

71Gou Gourdon, C., Marty, D., Maschke, E.K., Touche, J.: The Torsatron without Toroidal Field Coils as a Solution of the Divertor Problem, Nucl. Fus. **11** (1971) 161.

72Wob Wobig, H., Rehker, S.: A Stellarator Coil System without Helical Windings, Proc. 7th Symp. on Fusion Technology, Grenoble, France (October 24-27, 1972) 333.

74Iiy Iiyoshi, A., Uo, K.: Proc. 5th Inter. Conf. on Plasma Physics and Controlled Nuclear Fusion Research, IAEA-CN-33/G4, III (1974) 619.

76Geo Georgievskii, A.V., Loktionov, Yu.M., Suprunenko, V.A.: Characteristics of a Hypothetical Thermonuclear Stellarator Reactor in the 'Plateau' Regime, Kharkhov Physico-Technical Institute report KhFTI 76-38 (1976), English translation in UKAEA Culham Laboratory report CTO/1299 (1976).

78Miy Miyamoto, K.: Recent Stellarator Research, Nucl. Fus. **18** (1978) 243.

79Pol Politzer, P.A., Lidsky, L.M., Montgomery, D.B.: Torsatrons and the TOREX Proof of Principle Experiment, Massachusetts Institute of Technology report PFC/TR-79-1 (March 1979).

81And Anderson, D.T., Derr, J.A., Shohet, J.L.: IEEE Transactions on Plasma Science, PS-9 No. 4 (1981) 212.

81Gru Gruber, R. et al.: Comp. Phys. Com. **24** (1981) 364.

81Mil Miller, R.L., Krakowski, R.A.: The Modular-Stellarator Fusion Reactor Concept, Los Alamos National Laboratory report LA-8978 (August 1981).

82Bad Badger, B. et al.: University of Wisconsin Report UWFDM-550 (1982).

83Bro Brossmann, U., Dommaschk, W., Herrnegger, F., Grieger, G., Kißlinger, J., Lotz, W., Nührenberg, J., Rau, F., Renner, H., Ringler, H., Sapper, J., Schlüter, A., Wobig, H.: Concept of an Advanced Stellarator, Plasma Physics and Contr. Nucl. Fusion Research (Proc. 9th Int. Conf., Baltimore 1982), Vol. III (IAEA Vienna 1983) 141.

84Boo Boozer, A.: Phys. Fluids **27** (1984) 2110.

85Kis Kißlinger, J., Wobig, H.: Europhys. Conf. Abstracts,Vol. 9F Part I (1985) 453.

86Hir Hirshman, S.P., Shaing, K.C., van Rij, W.I., Beasly, C.O., Crume Jr., E.C.: Phys. Fluids **29** (1986) 2951.

86Nue Nührenberg, J., Zille, R.: Phys. Lett. **A 114** (1986) 129.

86Rei Reiman, A., Greenside, H.: Comp. Phys. Com. **43** (1986) 147.
87Boe1 Böhme, G. et al.: IPP-report IPP 2/285, KfK-report KfK 4268, Fusion Power Assoc./Univ. Wisc. FPA-87-2 (1987).
87Boe2 Böhme, G. et al.: IPP-Report 2/285 (1987).
87Mer Merkel, P.: Nuclear Fusion **27** (1987) 867.
87Nue Nührenberg, J., Zille, R.: Equilibrium and stability of low-shear stellarators, Proc. of the workshop on Theory of Fusion Plasmas, Varenna 1987, Editrice Compositori, Bologna 1987, EUR 11336 EN.
88Bei Beidler, C.D.: Proc. 2nd workshop on Wendelstein 7-X, EUR 11705 En (1988) 121.
88Nue Nührenberg, J., Zille, R.: Quasi-Helically Symmetric Toroidal Stellarators, Phys. Lett. **A 129** (1988) 113.
89Bei Beidler, C.D.: Proc. 16th European Conf. Contr. Fusion and Plasma Physics, Venice 1989, Vol. 13B, Part II (1989) 675.
89Har Harafuji, K., Hayashi, T., Sato, T.: J. Comp. Phys. **81** (1989) 169.
90Bei Beidler, C.D. et al.: Fusion Technology **17** (1990) 148.
90Hir Hirshman, S.P. et al. : J. Comp. Phys. **87** (1990) 396.
90Iiy Iiyoshi, A., Fujiwara, M., Motojima, O., Ohyabu, N., Yamazaki, K.: Fusion Technology **17** (1990) 169.
90Lac Lackner, K., Gottardi, E.: Nucl. Fusion **30** (1990) 767.
90Sap Sapper, J., Renner, H.: Fusion Technology **17** (1990) 62.
92Lot Lotz, W., Merkel, P., Nührenberg, J., Strumberger, E.: Plasma Phys. Control. Fusion **34** (1992) 1037.
93Naj Najmabadi, F., Conn, R.W. et al.: UCLA-Report UCLA-PPG-1461 (1993).
93Nue Nührenberg, C.: Phys. Fluids **B 5** (1993) 3195.
94Don dalle Donne, M.: European DEMO BOT solid breeder blanket, KfK-Report 5429 (1994).
95Mal Malang, S. et al.: Development of Self-Cooled Liquid Metal Breeder Blankets, FZKA 5581 (1995).
95Rae Raeder, J. et al.: Report of the SEAFP project EURFUBRU XII-217/95 (1995).
96Hen Hender, T.C., Knight, P.J., Cook, I.: 12th Topical Meeting on the Technology of Fusion Energy, ANS, Reno, Nevada (1996).
96Str Stroth, U., Murakami, M., Dory, R.A., Yamada, H., Okamura, S., Sano, F., Obiki, T.: Nucl. Fusion **36** (1996) 1063.
97UCS Stellarator power plant study, UCSD-ENG-004 (1997).
98Bei1 Beidler, C.D. et al.: IAEA Conf. on Controlled Fusion, IAEA-F1-CN-69/FTP/01, Yokohama (1998).
98Bei2 Beidler, C.D., Stroth, U., Wobig, H.: IPP-Report 2/338 (February 1998).
98Sag Sagara, A. et al.: Fus. Eng. Design **41** (1998) 349.
98Shi Shishkin, A.A., Sidorenko, I., Wobig, H.: IPP Report 2/340 (April 1998).
98Spo Spong, D.A. et al.: Phys. Plasmas **5** (1998) 1752.
98Wie Wieczorek, A., Zacharias, L.: Computer simulations of the power supply and the protection system for the superconducting coils of the fusion reactor, Proc. 5th European Power Quality Conf., Nürnberg (1998).
98Yam Yamanishi, H. et al.: Fus. Eng. Design **41** (1998) 583.
99Har Harmeyer, E., Kißlinger, J., Wobig, H.: IPP-Report III/241 (May 1999).
99Mal Malang, S.: Fus. Eng. Design **46** (1999) 193.
99Por Porfiri, M.T., Gambi, G., Pinna, T.: Functional failure mode and effect analysis for a stellarator power plant model, Report ERG FUS TN SIC 07/99 (1999).
99Str1 Strumberger, E., Nührenberg, C. et al.: Paper P4.031, Proc. 26th EPS-Conf., Maastricht (June 1999).
99Str2 Strumberger, E. et al.: IPP-Report III/249 (1999).

99Wob1 Wobig, H., Harmeyer, E., Herrnegger, F., Kißlinger, J.: Blanket Concepts of the Helias Reactor, IPP-Report III/244 (1999).
99Wob2 Wobig, H., Pfirsch, D.: IPP-Report III/245 (September 1999).
00Kis Kißlinger, J., Beidler, C.D., Wobig, H.: EPS-Conf. Budapest (2000).
00Tak Takeiri, Y. et al.: Proc. 12th Int. Toki Conf. on Plasma Phys. ad Contr. Fusion, Toki (January 2000).